UHASSELT
KNOWLEDGE IN ACTION

Maastricht University

Faculty of Medicine and Life Sciences
School for Life Sciences
Master of Biomedical Sciences

Master's thesis

Functional characterization of cardiac atrial appendage stem cells: focus on true cardiac repair after myocardial infarction

Hanne Beliën

Thesis presented in fulfillment of the requirements for the degree of Master of Biomedical Sciences, specialization Clinical Molecular Sciences

SUPERVISOR :
Prof. dr. Virginie BITO

MENTOR :
Mevrouw Lize EVENS

CO-SUPERVISOR :
Prof. dr. Annelies BRONCKAERS

2018
2019

Transnational University Limburg is a unique collaboration of two universities in two countries: the University of Hasselt and Maastricht University.

UHASSELT
KNOWLEDGE IN ACTION

www.uhasselt.be
Universiteit Hasselt
Campus Hasselt:
Martelarenlaan 42 | 3500 Hasselt
Campus Diepenbeek:
Agoralaan Gebouw D | 3590 Diepenbeek

UHASSELT
KNOWLEDGE IN ACTION

Maastricht University

Faculty of Medicine and Life Sciences
School for Life Sciences
Master of Biomedical Sciences

Master's thesis

Functional characterization of cardiac atrial appendage stem cells: focus on true cardiac repair after myocardial infarction

Hanne Beliën

Thesis presented in fulfillment of the requirements for the degree of Master of Biomedical Sciences, specialization Clinical Molecular Sciences

SUPERVISOR :
Prof. dr. Virginie BITO

MENTOR :
Mevrouw Lize EVENS

CO-SUPERVISOR :
Prof. dr. Annelies BRONCKAERS

Table of contents

Table of contents ..... **i**

Acknowledgements ..... **iii**

List of abbreviations ..... **v**

Abstract ..... **vii**

Samenvatting ..... **ix**

1 Introduction **1**

1.1 Myocardial infarction 1

1.1.1 Pathophysiology of myocardial ischemia 2

1.1.2 Current therapeutic strategies 4

1.2 Regenerative stem cell therapy for myocardial infarction 5

1.2.1 Skeletal myoblasts 5

1.2.2 Mesenchymal stem cells 6

1.2.3 Induced pluripotent stem cells 6

1.2.4 Cardiac progenitor cells 7

1.3 Cardiac Atrial Appendage Stem Cells 8

1.4 Stimulating CASCs properties for true cardiac repair 9

2 Materials and methods **11**

2.1 Experimental protocol 11

2.2 Lentiviral vector production 11

2.3 CASCs isolation and expansion 12

2.4 Induction of myocardial infarction 13

2.5 Evaluation of *in vivo* cardiac function 13

2.5.1 Conventional echocardiography 13

2.5.2 Hemodynamic measurements 14

2.6 Cardiomyocyte isolation and unloaded cell shortening 14

2.7 Fibrosis measurement 14

2.8 Immunohistochemistry 15

2.9 Propidium iodide assay 15

2.10 Transwell migration assay 16

2.11 Reverse transcriptase PCR 16

2.12 Statistics 17

3 Results **19**

3.1 CASCs transplantation improves echocardiographic and hemodynamic parameters after MI 19

3.2 CASCs transplantation restores resident cardiomyocyte shortening and kinetics 23

3.3 Interstitial collagen deposition tends to decrease after CASCs transplantation 25

3.4 CASCs could not be identified in cardiac tissue 26

3.5 Conditioned medium of DPSCs promotes CASCs proliferation and survival 27

3.6 Conditioned medium of DPSCs promotes CASCs migration 28
3.7 CASCs genetically express VEGFR1 28
4 Discussion 29
4.1 CASCs transplantation improves *in vivo* cardiac function after MI 29
4.2 CASCs transplantation improves resident cardiomyocyte contractility 32
4.3 CASCs transplantation reduces cardiac fibrosis 33
4.4 CASCs engraftment in cardiac tissue is limited 33
4.5 What is the effect of Matrigel on cardiac repair? 34
4.6 Conditioned medium of DPSCs boosts CASCs functional properties *in vitro* 35
4.7 Limitations and future perspectives 36
5 Conclusion 39
6 References 41

Acknowledgements

During my last year in Biomedical Sciences, I conducted my senior internship at BIOMED in the cardiology group. Performing experiments and writing this thesis would not have been possible without the aid and support of several people.

First I would like to express my sincere gratitude to my promotor prof. dr. Virginie Bito for giving me the opportunity to conduct my senior internship in the cardiology group. Virginie, thank you for all the advice and suggestions you gave me during this project and for always finding new solutions whenever there was a problem. You provided me with constructive feedback and criticism, without which it was impossible to accomplish my thesis. With your enthusiasm and passion for cardiology, you taught me the delight of studying cardiophysiological diseases. There is no way to express how much it means to me to have been a member of the cardiology team!

I would especially like to thank my daily supervisor Lize Evens for teaching me what a hard-working scientist can accomplish. Thank you for your continuous support and for all the experience you gave me during this internship. You were always there to answer my questions and to give me feedback on the practical and theoretical level. You inspired me to become an independent researcher and to develop myself further in the scientific field. I did not only enjoy our scientific discussions, but also our less scientific conversations. Thank you for being such a great and helpful supervisor!

My sincere thanks also go to my second examiner prof. dr. Annelies Bronckaers for always having time to answer my questions and for giving advice and suggestions during this project. I would also like to thank the morphology group for the support with the transwell and propidium iodide experiments.

Next, I am grateful to Dorien Deluyker, Maxim Verboven and all other members of the physiology group for giving feedback and helping with experiments during my internship.

I would also like to thank my fellow students for listening to each other's stories and for all the joyful moments during lunches and coffee breaks. Finally, I want to thank my family and friends for continuously supporting and encouraging me throughout the years and during this internship.

List of abbreviations

ACE	Angiotensin-converting enzyme
ALDH	Aldehyde dehydrogenase
ANG1	Angiopoietin-1
ARB	Angiotensin II receptor blocker
AWT	Anterior wall thickness
CABG	Coronary artery bypass graft
CASC	Cardiac atrial appendage stem cell
CDCs	Cardiosphere-derived cells
CM	Conditioned medium
CO	Cardiac output
cTn	Cardiac troponin
cTnI	Cardiac troponin I
cTnT	Cardiac troponin T
Cx43	Connexin43
DAPI	4',6-diamidino-2-phenylindole
DEAB	Diethylaminobenzaldehyde
DMEM	Dulbecco's modified eagle medium
dP/dt_{max}	Peak rate of pressure rise
dP/dt_{min}	Peak rate of pressure decline
DPSC	Dental pulp stem cell
ECAE	Ethical Committee for Animal Experimentation
ECG	Electrocardiogram
ECM	Extracellular matrix
EDP	End-diastolic pressure
EDV	End-diastolic volume
EF	Ejection fraction
EGF	Epidermal growth factor
ESV	End-systolic volume
FCS	Fetal calf serum
FGF2	Fibroblast growth factor-2
FITC	Fluorescein isothiocyanate
GAPDH	Glyceraldehyde 3-phosphate dehydrogenase
GFP	Green fluorescent protein
HBSS	Hank's Balanced Salt Solution
HR	Heart rate
HRP	Horseradish peroxidase
HSC	Hematopoietic stem cell
IGF-II	Insulin-like growth factor-II
IHD	Ischemic heart disease
IL-1β	Interleukin 1β
IL-6	Interleukin 6
iPSC	Induced pluripotent stem cell
isl1	Islet-1

L/L_0	Fractional shortening
LAD	Left anterior descending
LV	Left ventricle
LVEDD	Left ventricular end-diastolic diameter
LVESD	Left ventricular end-systolic diameter
LVIDD	Left ventricular inner diastolic diameter
LVISD	Left ventricular inner systolic diameter
LVP	Left ventricular pressure
MHC	Myosin heavy chain
MI	Myocardial infarction
MLC-2V	Ventricular myosin light chain 2
MMP	Matrix metalloproteinase
MSC	Mesenchymal stem cell
NSTEMI	Non-ST-segment elevation myocardial infarction
OD	Optical density
P/S	Penicillin/streptomycin
P1	Passage 1
PBS	Phosphate-buffered saline
PBS-T	PBS-Triton
PCI	Percutaneous coronary intervention
PFA	Paraformaldehyde
PI	Propidium iodide
PWT	Posterior wall thickness
RAAS	Renin-angiotensin-aldosterone system
ROS	Reactive oxygen species
RT_{50}	Half time relaxation
RT-PCR	Reverse transcriptase polymerase chain reaction
Sca-1	Stem cell antigen-1
SEM	Standard error of the mean
SNS	Sympathetic nervous system
STEMI	ST-segment elevation myocardial infarction
SV	Stroke volume
Tau	Relaxation time constant
TGF-β	Transforming growth factor β
TIMP	Tissue inhibitor of metalloproteinases
TMB	Tetramethylbenzidine
TNF-α	Tumor necrosis factor α
TTP	Time to peak
VEGF	Vascular endothelial growth factor
VEGFR	Vascular endothelial growth factor receptor
α-MEM	Minimal essential medium, alpha modification

Abstract

Introduction: Myocardial infarction (MI) is the leading cause of heart failure worldwide. Recent therapies are unable to replace lost cardiac tissue after MI and can thereby not prevent progression towards heart failure. Our research group recently identified a new cardiac stem cell type, the cardiac atrial appendage stem cells (CASCs), with superior cardiomyogenic differentiation potential *in vitro* compared to other stem cells. Nevertheless, functional improvement in cardiac function at the organ and cellular level as well as differentiation of CASCs after *in vivo* transplantation still needs to be confirmed before translating this therapy to the clinic. In addition, the application potential of CASCs is limited by poor cell engraftment due to low survival and proliferation of CASCs in the hostile ischemic environment. Therefore, dental pulp stem cells (DPSCs), which exert strong paracrine and cytoprotective effects, were used to boost CASCs functional properties, aiming at true cardiac repair after MI.

Material & methods: Chronic MI was performed in female rats receiving either no injections or injections with CASCs in the infarction border zone of the heart. Four weeks after surgery, global cardiac function was assessed by echocardiographic and hemodynamic measurements. Single cardiomyocytes were isolated from the left ventricle and unloaded cell shortening of resident cardiomyocytes was assessed at 1, 2 and 4 Hz. Cardiac fibrosis was measured using a collagen staining. CASCs engraftment was assessed by immunohistochemical staining. The effect of DPSCs on CASCs proliferation, viability and migration was investigated *in vitro* with propidium iodide, transwell migration and reverse transcriptase PCR assays.

Results: CASCs transplantation improved *in vivo* cardiac function after MI as demonstrated by the significant increase in ejection fraction and anterior wall thickness and the significant decrease in end-systolic volume and cardiac diastolic pressures. In addition, CASCs transplantation significantly restored resident cardiomyocyte shortening and kinetics. Interstitial collagen deposition tended to decrease after CASCs therapy. Finally, conditioned medium of DPSCs significantly stimulated CASCs proliferation, survival and migration *in vitro*.

Discussion and conclusion: Our data indicate that CASCs transplantation improves cardiac function after MI both at the organ and cellular level despite limited CASCs engraftment. Additionally, we show that preconditioning of CASCs with DPSCs promotes CASCs functional properties. Altogether, this study shows the efficacy of CASCs therapy after MI.

Samenvatting

Introductie: Myocardinfarct (MI) is wereldwijd de meest frequente oorzaak van hartfalen. Huidige therapieën kunnen het beschadigde cardiale weefsel niet herstellen en bijgevolg de verdere progressie naar hartfalen niet verhinderen. Onze onderzoeksgroep heeft recent een nieuwe cardiale stamcel, 'cardiac atrial appendage stem cells' (CASCs), ontdekt met een hogere *in vitro* differentiatiecapaciteit naar cardiomyocyten vergeleken met andere stamcellen. Zowel functionele verbetering in cardiale functie op orgaan- en celniveau, als differentiatie van CASCs na *in vivo* transplantatie moeten echter nog bevestigd worden voordat deze therapie in het ziekenhuis gebruikt kan worden. Daarnaast zijn de toepassingsmogelijkheden van deze stamcellen beperkt door de lage celretentie aangezien CASCs een beperkte mogelijkheid hebben om te overleven en prolifereren in de ischemische omgeving van het infarct. Dentale pulp stamcellen (DPSCs) hebben sterke paracriene en celbeschermende eigenschappen en werden daarom in deze studie gebruikt om de functionele eigenschappen van CASCs te stimuleren.

Materiaal en methoden: Vrouwelijke ratten met een chronisch MI werden ofwel geïnjecteerd met CASCs in de peri-infarct regio van het hart of kregen geen injecties. Vier weken na de operatie werd globale cardiale functie bepaald met echocardiografie en hemodynamische metingen. Individuele cardiomyocyten werden geïsoleerd uit het linker ventrikel om de contractie van residente cardiomyocyten te meten op 1, 2 en 4 Hz. Cardiale fibrose werd gemeten door middel van een collageenkleuring. CASCs retentie werd nagegaan met een immunohistochemische kleuring. Het effect van DPSCs op CASCs proliferatie, overleving en migratie werd *in vitro* onderzocht met een propidium jodide, transwell migratie en reverse transcriptase PCR assay.

Resultaten: CASCs transplantatie verbeterde de *in vivo* cardiale functie na MI door enerzijds ejectie fractie en anterieure wanddikte significant te verhogen en anderzijds het eind-systolisch volume en de diastolische cardiale drukken significant te verlagen. Bovendien herstelde CASCs transplantatie de contractie en kinetiek van de reeds aanwezige cardiomyocyten. Interstitieel collageen verminderde na CASCs therapie. Tenslotte zorgde geconditioneerd medium van DPSCs voor een significante verbetering in proliferatie, overleving en migratie van CASCs *in vitro*.

Discussie en conclusie: Onze resultaten tonen aan dat CASCs transplantatie de cardiale functie na MI verbetert op orgaan- en celniveau ondanks de beperkte CASCs retentie. Daarnaast tonen wij aan dat stimulatie van CASCs met DPSCs de functionele eigenschappen van CASCs bevordert. Uit deze studie kunnen we concluderen dat CASCs transplantatie een effectieve therapie is na MI.

1 Introduction

1.1 Myocardial infarction

Ischemic heart disease (IHD) is the leading cause of global mortality, accounting annually for more than 7 million deaths worldwide in the last 15 years (1). This disease was described first in 1772 by the British physician William Heberden, who noted that patients experienced a discomfort in the chest during physical activities. Today, IHD is defined as the imbalance between myocardial oxygen supply and demand, and it is subdivided in a spectrum of syndromes based on the clinical manifestation (2). Myocardial infarction (MI), or better known as heart attack, is one of the most well-known clinical manifestations of IHD. The term MI is used in case of acute myocardial injury due to ischemia. MI is caused by the prolonged interruption of the coronary blood supply. In this condition, an insufficient amount of oxygen and nutrients is delivered to the myocardium. Together with accumulation of reactive oxygen species (ROS), inflammatory proteins and metabolites within the cardiac tissue, this results in myocardial cell death (2-5). Patients who experience MI mostly present with a variety of symptoms including discomfort in the chest, upper extremities and mandibles in combination with dyspnea and nausea. However, sometimes atypical symptoms, such as palpitations or cardiac arrest, may be present during MI. Some patients even manifest without symptoms (3). More women than men present clinically with atypical symptoms like fatigue, sleep disturbances, anxiety and arm weakness (5). Overall, the incidence of men affected by MI is two times higher than that of women, because women benefit from the cardioprotective effects of estrogens (6). Besides that, women develop MI on average seven to ten years later than men due to their lower level of risk factors before the age of 60 (5, 7). The diagnosis of MI is based on electrocardiogram (ECG) changes together with the detection of myocardial cell death (3-5). During myocardial ischemia, changes in the ST segment and T wave of the ECG are generally observed and depend on the severity of the coronary occlusion. A partial occlusion of the coronary artery leads to subendocardial ischemia and results in ST segment depression and T wave flattening or inversion, referred to as non-ST-segment elevation myocardial infarction (NSTEMI). In case the coronary artery is completely occluded, ST-segment elevations are observed in the ECG suggesting a more severe transmural myocardial ischemia, referred to as ST-segment elevation myocardial infarction (STEMI) (2). Myocardial cell death is detected by the leakage of the myofilament protein cardiac troponin (cTn) from damaged cardiomyocytes into the bloodstream. Elevated blood levels of cTn above the upper reference limit of normal, which depends on the manufacturer and the troponin assay that is used (8), is an essential indicator for the diagnosis of MI (4).

1.1.1 Pathophysiology of myocardial ischemia

Myocardial ischemia is the result of the imbalance between myocardial oxygen supply and demand, and it can be caused by several conditions. First, there are conditions that decrease the myocardial oxygen supply. These include reduced myocardial blood flow due to atherosclerosis of the coronary arteries, reduced perfusion pressure as a result of hypotension or septic shock, and a large reduction in blood oxygen content due to anemia or impaired blood oxygenation by the lungs. On the other hand, conditions that increase myocardial oxygen demand can induce myocardial ischemia, such as ventricular tachyarrhythmias, acute hypertension, and severe aortic stenosis (2, 3). MI most often results from atherosclerosis of the coronary arteries, leading to prolonged interruption of the coronary blood supply of the heart (Figure 1). Atherosclerosis is a progressive, inflammatory process that may occur in all arteries of the body and in which normal homeostasis of the arterial wall is disturbed (2).

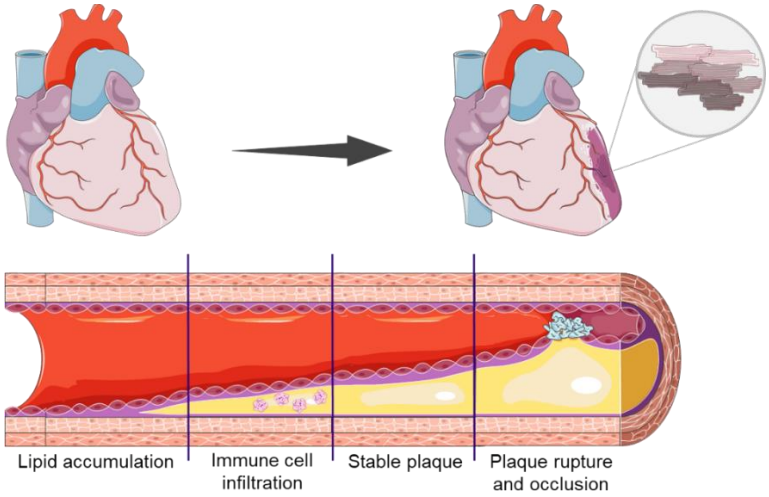

Figure 1: Pathogenesis of myocardial infarction. Progressive development of atherosclerosis in the coronary arteries eventually leads to plaque rupture and coronary occlusion, thereby causing myocardial ischemia and cardiomyocyte death.

The most common risk factors to develop atherosclerosis are related to a sedentary lifestyle, such as low physical activity, smoking, alcohol use, obesity, and a high-risk diet containing a high level of saturated fatty acids and trans-fatty acids, salt and sugar (such as snacks, meat and butter). Other risk factors include hypertension, hyperlipidemia, diabetes mellitus, family history of cardiovascular disease, increasing age and gender (7). Disturbance of arterial homeostasis leads to endothelial dysfunction, causing lipid accumulation and modification underneath the endothelial cells. Both immune cells and smooth muscle cells infiltrate the arterial wall, after which foam cells are formed and extracellular matrix proteins are deposited (2). As a result, stable plaques are formed containing a small lipid core and a thick fibrous cap, thereby narrowing the coronary artery lumen. Patients with stable plaques may experience chest discomfort when myocardial oxygen demand is increased, such

as during physical activity, which is referred to as *stable angina*. A stable plaque can evolve towards a vulnerable plaque, consisting of a large lipid core and thin fibrous cap. These plaques tend to rupture, resulting in thrombus formation and occlusion of the coronary artery (2, 9, 10). The reduction in myocardial blood supply causes an insufficient delivery of oxygen and nutrients to the myocardium, and an accumulation of ROS, inflammatory proteins and metabolites within the cardiac tissue. Myocardial ischemia of 15-20 minutes is sufficient to induce irreversible changes in cardiomyocyte structure, resulting in irreversible myocardial cell death (2, 3, 9). Death of cardiomyocytes stimulates a cardiac repair process consisting of an inflammatory phase, a proliferative phase and a maturation phase (9, 11). In the inflammatory phase, damaged cardiomyocytes release a range of signals, such as pro-inflammatory cytokines including interleukin 1β (IL-1β), tumor necrosis factor α (TNF-α) and interleukin 6 (IL-6), to activate and attract leukocytes to the infarct area. Infiltrated leukocytes clear the infarcted myocardium from dead cells and extracellular matrix debris, thereby repressing the pro-inflammatory response resulting in the transition to the proliferative phase. During the proliferative phase, resident cardiac fibroblasts located in the extracellular matrix of the heart are activated to transdifferentiate into myofibroblasts characterized by a proliferative, matrix-synthetic phenotype (9, 11). Activation of cardiac fibroblasts is mediated by increased levels of transforming growth factor β (TGF-β) in the infarcted myocardium, changes in the extracellular matrix composition and activation of the renin-angiotensin-aldosterone system (RAAS) (11). Myofibroblasts are responsible for the increased deposition of extracellular matrix proteins, such as collagen type I and fibronectin, thereby altering the composition of the extracellular matrix. In addition, inhibition of matrix metalloproteinases (MMPs) and activation of tissue inhibitor of metalloproteinases (TIMPs) shifts the balance to extracellular matrix protein synthesis, leading to the formation of a scar tissue. Finally, the maturation phase of cardiac repair is characterized by cross-linking of the extracellular matrix and inactivation of cardiac myofibroblasts, thereby stabilizing the scar tissue (9, 11). The overall process of cardiac repair after MI, starting from cardiomyocyte cell death until scar stabilization, lasts approximately 3-4 weeks (11). Because the heart has minimal regenerative capacity, scar tissue formation in the infarcted area remains irreversible and impairs normal heart function (9, 11). The disturbances in cardiac contraction and relaxation are counteracted by compensatory mechanisms in the non-infarcted myocardium that ensure perfusion of vital organs (12-14). These compensatory mechanisms are driven by neurohormonal pathways that activate the sympathetic nervous system (SNS) and RAAS, leading to adverse ventricular remodeling characterized by hypertrophy. Eventually, the compensatory mechanisms cannot maintain cardiac function within its normal range, causing dilatation of the ventricular chamber out of proportion to the wall thickness (13, 14). Over time, cardiac function continues to decline and reaches a point where the heart is not able to meet the metabolic demands of the body, thereby ending at the stage of heart failure (12).

1.1.2 Current therapeutic strategies

Therapy of MI aims to restore the balance between myocardial oxygen supply and demand, and to prevent recurrent infarctions (2, 9). Administration of β-blockers after MI improves the myocardial oxygen balance by reducing oxygen demand. Inhibition of the β-adrenergic response decreases ventricular contractility and slows down the heart rate, resulting in relief of ischemia by reducing myocardial oxygen consumption and by increasing the time for coronary perfusion. In addition, organic nitrates are administered to patients with MI both to decrease myocardial oxygen demand and to increase oxygen supply (2). Nitrates induce venous dilatation that diminishes preload and ventricular filling, and as such ventricular wall stress, to reduce myocardial oxygen consumption. Furthermore, coronary dilatation by nitrates increases myocardial perfusion and oxygen supply. Revascularization of the coronary artery is often pursued to restore the coronary blood supply and to reduce the risk of recurrent infarctions, thereby improving patient survival after MI (9, 15). Revascularization therapy can be subdivided in the percutaneous coronary interventions (PCIs) to re-open the occluded coronary artery (such as conventional balloon angioplasty and coronary stent implantation), the coronary artery bypass graft (CABG) surgeries to bypass the obstructed coronary artery, and fibrinolytic therapy to break down the coronary blood cloth (2, 5).

To prevent reinfarctions in the long-term, therapies focus mainly on the control of vulnerable plaques in patients with coronary atherosclerosis. Change of lifestyle is a key factor in the long-term therapy of MI. Lifestyle interventions include stimulation of physical activity, diet and weight control, smoking cessation, alcohol restriction and blood pressure control (5). In addition to changes in lifestyle, lipid-lowering therapy, such as statins, also reduces recurrent infarctions and mortality in patients with established atherosclerosis. The mechanism of action by which lipid-lowering agents improve patient outcome is broader than the lipid-altering effect alone. These drugs also reduce inflammation of the vascular wall and improve endothelial cell function (2, 9). Since thrombus formation is the main aspect in the pathophysiology of MI, antithrombotic therapy is provided to stabilize the vulnerable plaque and to prevent coronary reocclusion (2, 16). Antithrombotic therapy consists of two components: antiplatelet therapy to target platelet activation and aggregation, and anticoagulant therapy to prevent clot formation (16).

After MI, disturbances in cardiac function result in adverse ventricular remodeling, eventually leading to heart failure. As such, therapeutics that slow down ventricular remodeling are administered after MI. In addition to the positive effect of β-blockers on myocardial oxygen balance, β-blockers also have a positive effect on adverse ventricular remodeling after MI by counteracting the overstimulation of the SNS (13). Angiotensin-converting enzyme (ACE) inhibitors and angiotensin II receptor blockers

(ARBs) positively affect cardiac remodeling as well by counteracting activation of the RAAS. However, current therapies are unable to restore the damaged cardiac tissue and, as such, can only delay progression towards heart failure (5). The last therapeutic option for heart failure patients is cardiac transplantation, but this procedure has a high post-transplantation mortality and only low numbers of donor hearts are available, meaning that not all patients can receive a heart transplant (17). Therefore, new approaches are needed to regenerate lost cardiomyocytes in the infarcted area.

1.2 Regenerative stem cell therapy for myocardial infarction

For a long time, it was believed that the heart cannot regenerate the damaged myocardium after injury. This notion was, however, rejected at the beginning of this century by the discovery of cardiomyocyte proliferation in mammalian hearts (9, 18, 19). Endogenous regeneration is a rare event and is insufficient to repair all millions of lost cardiomyocytes in the infarcted tissue (20). Therefore, new methods to enhance the intrinsic repair processes of the heart are currently under investigation, which triggered the search for the most appropriate stem cell type to regenerate myocardium (Figure 2) (20-22).

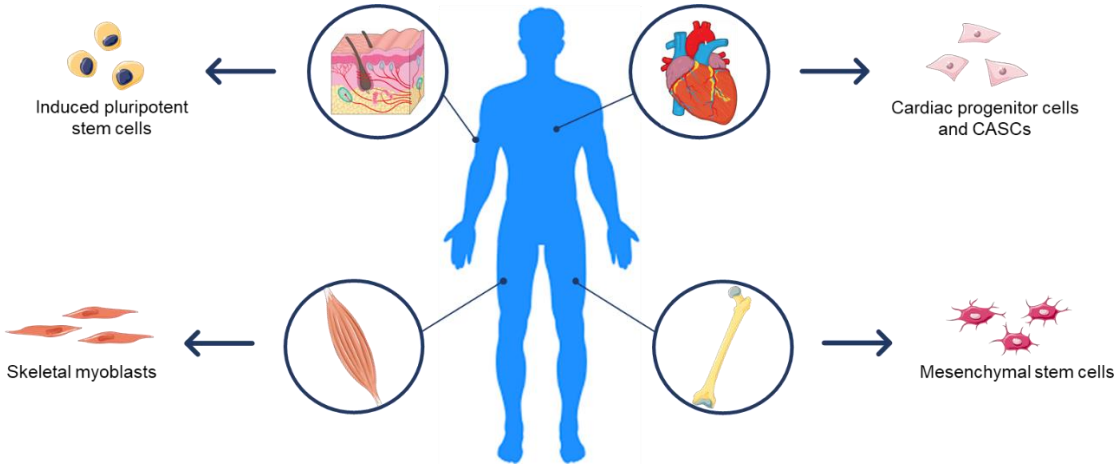

Figure 2: Stem cell types for myocardial regeneration. Stem cell candidates for regeneration of injured myocardium and their source in the human body. CASCs, cardiac atrial appendage stem cells.

1.2.1 Skeletal myoblasts

In an attempt to repair cardiac tissue, the first preclinical and clinical studies focused on undifferentiated skeletal muscle-derived myoblasts, also referred to as satellite cells (21, 22). Skeletal myoblasts, harvested from muscle biopsies, showed differentiation into cardiomyocyte-like cells upon transplantation in a canine model of myocardial cryoinjury (23). These findings initiated clinical trials in which autologous skeletal myoblasts were intramyocardially injected in patients with MI (24). Although the first clinical studies reported a significant improvement in cardiac function, subsequent

trials in a large number of patients failed to report an improved cardiac function and revealed ventricular arrhythmias after myoblast transplantation (25, 26). These negative results suggest that skeletal myoblasts have a low engraftment in cardiac tissue and lack the electromechanical coupling with cardiomyocytes, such as the cell junction protein connexin43 (Cx43) (27).

1.2.2 Mesenchymal stem cells

In order to find the ideal stem cell for cardiac regeneration, the focus was shifted towards bone marrow-derived cells, including mononuclear cells, endothelial progenitor cells, hematopoietic stem cells (HSCs), and mesenchymal stem cells (MSCs). Clinical trials transplanting mononuclear cells after MI showed limited functional improvement of the heart, and this small improvement was probably due to positive paracrine effects rather than differentiation of mononuclear cells into cardiomyocytes (28, 29). Furthermore, preclinical data demonstrated that endothelial progenitor cells co-cultured with rat neonatal cardiomyocytes could not transdifferentiate into cardiomyocytes (30). In addition, HSCs cannot transdifferentiate into cardiomyocytes and are, therefore, not suitable as a therapy for cardiac ischemic injury (31, 32).

MSCs are multipotent stem cells that can differentiate into all tissues of the mesoderm, including adipose tissue, bone, and cartilage. Because muscle tissue is also part of the mesoderm, MSCs were considered to be the most appropriate stem cell type for cardiomyogenic differentiation (33). MSCs reside in all adult stromal tissues, but are mainly isolated from bone marrow and adipose tissue for cardiac applications (22, 33). Isolation of MSCs is based on their fibroblast morphology, their adherence to plastic, the expression and absence of specific surface markers, and their trilineage differentiation capacity into adipocytes, osteoblasts and chondrocytes (33). MSCs have low immunogenic properties and are able to migrate to the site of injury (34). In this regard, clinical trials injecting MSCs in patients with MI were initiated (35, 36). Although global symptom scores were improved, no significant changes in cardiac function were observed due to the restricted engraftment and the lack of cardiomyogenic differentiation of MSCs (31, 37). As such, the benefit of MSCs is likely due to paracrine effects rather than the generation of *de novo* cardiomyocytes (22).

1.2.3 Induced pluripotent stem cells

Another potential candidate for cell-based regeneration of injured myocardium is the use of induced pluripotent stem cells (iPSCs). iPSCs are pluripotent stem cells created from adult somatic cells by nuclear reprogramming, a process in which the genes Oct4, Sox2, Klf4, and c-Myc are introduced into these cells (38). iPSCs can differentiate into all three germ layers and can, in theory, form every cell type of the body (22). Preclinical studies using iPSCs as a regenerative therapy for MI demonstrated

that iPSCs are able to differentiate into cardiomyocytes and to improve cardiac function (39). However, the pluripotent properties of iPSCs led to the formation of teratomas, indicating that this risk should be overcome before translating the iPSC technology to the clinic (40).

1.2.4 Cardiac progenitor cells

Despite previous disappointing results, the search for a cell-based regenerative therapy continued by exploring the cardiomyogenic differentiation potential of resident cardiac progenitor cells. Since these cells originate from the heart and may be 'pre-programmed' to become cardiomyocytes, they are considered to be more suitable for cardiac regeneration (37). Several endogenous stem cell populations were reported in the adult heart based on the expression of specific surface markers, such as islet-1 (isl1) (41), stem cell antigen-1 (Sca-1) (42), and MDR-1/ABCG2 (cardiac side population cells) (43). Next to that, the most well-studied cardiac stem cell types are the c-kit$^+$ cells and the cardiosphere-derived cells. Isolation of c-kit$^+$ cells, discovered by the group of P. Anversa, is based on the expression of the c-kit receptor (44). The use of this isolation method has some limitations: interaction of the antibody to the c-kit receptor is susceptible to non-specific binding, and binding to the receptor may alter cellular properties (37, 45). A first clinical trial, using intracoronary infusion of c-kit$^+$ cells, showed an increase in left ventricular (LV) systolic function and a decrease in infarct size (46). However, after other researchers failed to replicate P. Anversa's findings, investigations were started and have concluded that publications of P. Anversa contained falsified or fabricated data, leading to the retraction of 31 papers (47). Recently, it was shown that c-kit$^+$ cells only minimally (less than 0.03%) differentiate into new cardiomyocytes (48). Moreover, c-kit$^+$ cells in the heart were specifically identified as mast cells and are, as such, not able to regenerate myocardium (49).

Several research groups started to focus on the functional stem cell characteristic of sphere formation rather than the expression of surface markers. The formation of cardiospheres from atrial or ventricular biopsies resulted in the outgrowth of the so-called cardiosphere-derived cells (CDCs) (50). A clinical study was initiated using intracoronary infusion of CDCs, showing a reduction in scar size. Nevertheless, overall cardiac function was not significantly improved by CDCs therapy due to limited differentiation capacity into functional cardiomyocytes (37, 51). Moreover, it seems that sphere formation is not a unique stem cell marker for cardiac progenitor cells, but also for MSCs and myofibroblasts, and that cardiospheres are formed by aggregation of cells rather than cell cloning. Therefore, using sphere formation as a single stem cell marker may be an inaccurate isolation method (52).

1.3 Cardiac Atrial Appendage Stem Cells

Another promising method to isolate stem cells is based on a high aldehyde dehydrogenase (ALDH) enzyme activity. ALDH is a general stem cell marker and is also used as a marker for several stem cell types including mesenchymal, hematopoietic and neural stem cells (45, 53, 54). Although it is not entirely understood why high ALDH activity is beneficial for stem cell properties, it is known that ALDH enzymes metabolize toxic aldehydes to protect the cell (55). This indicates that stem cells expressing ALDH may be better protected against cytotoxic responses, for example in ischemia (45). Additionally, ALDH enzymes are involved in retinoic acid production, which is important for stem cell differentiation (55).

By using high ALDH activity, a new $ALDH^{+}CD34^{+}CD45^{-}$ cardiac stem cell type was recently identified in human atrial appendages and was therefore called "cardiac atrial appendage stem cell" (CASC) (45). To evaluate whether CASCs are able to regenerate cardiac tissue after MI, the cardiomyogenic differentiation capacity of CASCs was investigated. A first *in vitro* study of CASCs co-cultured with neonatal rat cardiomyocytes showed differentiation of CASCs towards a cardiac phenotype, which was observed by the gene expression of specific cardiomyocyte markers: cardiac troponin T (cTnT), myosin heavy chain (MHC), α-actinin, Cx43, potassium voltage-gated channel Kv4.3, L-type calcium channel subunit α1c and transcription factor GATA-4. In addition, differentiated CASCs expressed proteins such as cTnT and cardiac troponin I (cTnI). Interestingly, CASCs in co-culture also showed electrophysiological properties corresponding to that of mature cardiac cells (45). Subsequent experiments transplanting CASCs after acute MI in a mini-pig model confirmed the effectiveness of CASCs therapy *in vivo* (56). It was shown that CASCs reduce scar formation and preserve cardiac function after MI. These beneficial effects, in particular the preservation of cardiac function, were the result of engraftment of CASCs in the native cardiac tissue. After *in vivo* transplantation, differentiated CASCs expressed cardiac proteins such as cTnT, cTnI, and Cx43. Furthermore, CASCs transplanted in the left ventricle (LV) expressed proteins specific for ventricular cardiomyocytes (ventricular myosin light chain 2, MLC-2V), suggesting that CASCs, which originate from the atria, may differentiate towards a ventricular phenotype. These results demonstrate that CASCs have a greater cardiomyogenic differentiation potential compared to other stem cells already investigated in the treatment of MI (56). Besides that, CASCs stimulate angiogenesis via paracrine mechanisms, thereby further improving heart function after ischemia (57).

CASCs express several pluripotency-associated genes such as Oct-4, Nanog, c-Myc, Klf4, lin-28, DPPA3, and Tbx3 even after long-term *ex vivo* expansion, indicating that CASCs maintain important stem cell characteristics making them suitable for clinical applications. Although pluripotency is often associated

with tumor formation (40), no tumors were formed upon *in vivo* transplantation of CASCs in the mini-pig model and in nude mice (45). Moreover, stem cell transplantation in cardiac tissue is frequently related to arrhythmias (58), but no cardiac arrhythmias were detected by continuous rhythm analysis and ECG monitoring after CASCs therapy (56). This indicates that CASCs do not only have structural and functional advantages over other stem cells in cardiac repair, but are also considered to be a safe treatment.

Although some beneficial effects of CASCs on cardiac function have already been demonstrated *in vivo*, functional improvement in cardiac outcome should be confirmed at the organ and cellular level. Furthermore, it is not known whether CASCs will differentiate into true functional ventricular cardiomyocytes after repopulating the infarcted ventricular tissue. To date, only the expression of several cardiac proteins by differentiated CASCs have been examined after *in vivo* transplantation (56). However, functional characterization of differentiated CASCs is incomplete and only performed *in vitro* (45). As such, true differentiation of CASCs after *in vivo* transplantation still needs to be confirmed before translating this therapy to the clinic. Therefore, we hypothesize that CASCs improve cardiac function at the organ and cellular level by *in vivo* differentiation in functional ventricular cardiomyocytes in a rat model of MI. This study first aims to investigate the effect of CASCs transplantation on *in vivo* cardiac function. Second, the effect of CASCs transplantation on resident cardiomyocyte function and cardiac fibrosis will be examined. Finally, *in vivo* differentiated CASCs will be completely characterized by evaluating their structural and functional properties.

1.4 Stimulating CASCs properties for true cardiac repair

Current clinical trials using stem cells to replace lost cardiac tissue remain suboptimal, leading to disappointing results. The limiting therapeutic potential of many stem cell approaches is not only caused by the lack of stem cell differentiating properties, but is also due to the rather poor cell retention observed in any cell-based approach for regenerative medicine (59). Therefore, new regenerative therapies for MI should combine true cardiac tissue replacement with increasing cell retention and engraftment. One reason for the poor engraftment of transplanted cells in the hostile ischemic environment is the limited survival and proliferation of stem cells in the injured tissue. Dental pulp stem cells (DPSCs), a stem cell population isolated from the soft pulp tissue of teeth (60), have already demonstrated to efficiently improve cardiac function after MI with their strong paracrine properties (61). DPSCs secrete a broad range of paracrine factors such as vascular endothelial growth factor (VEGF), angiopoietin-1 (ANG1) and fibroblast growth factor-2 (FGF2) and it was recently shown that DPSCs exert even stronger paracrine and cytoprotective effects than bone marrow-derived MSCs (62, 63). Therefore, this study aims to combine the cardiomyogenic differentiating properties of CASCs

and the paracrine stimulating properties of DPSCs to truly replace lost cardiac tissue. We hypothesize that DPSCs can boost CASCs functional properties and their retention by creating a less hostile environment. First, the effect of DPSCs on CASCs proliferation, viability and migration will be investigated. Second, the first steps will be taken in elucidating the mechanisms by which DPSCs can boost CASCs properties.

2 Materials and methods

2.1 Experimental protocol

All animal experiments were conducted in accordance with the EU Directive 2010/63/EU for animal experiments and were approved by the local Ethical Committee for Animal Experimentation (ECAE) of Hasselt University, Belgium. Female Sprague-Dawley rats (n = 36, JANVIER LABS, Saint Berthevin Cedex, France), weighing 125 – 150 g at the start of the experiment, were randomly assigned into 3 groups undergoing surgery (SHAM, MI or MI with green fluorescent protein-labeled CASCs). All animals were maintained in standard cages in a controlled environment with reversed 12 h day/night cycle and received food and water *ad libitum*. At sacrifice (4 weeks postoperative), non-invasive echocardiographic and invasive hemodynamic measurements were performed. Blood samples were obtained at baseline, 24 h after surgery to confirm MI and at sacrifice. After harvesting the hearts, single cardiomyocytes were isolated from the LV by enzymatic dissociation through retrograde perfusion of the aorta for unloaded cell shortening measurements. In addition, transversal sections of the LV were fixed in 4% paraformaldehyde (PFA) for 24 h and placed in 30% sucrose for cryopreservation. After 24 h, tissues were embedded in Frozen Section Compound (Leica Microsystems, Diegem, Belgium) for storage at –80 °C until staining. Due to the experimental set-up, the number of animals used in each experiment is not equal to the total number of animals in this study. The exact number of animals that is used in each experiment is indicated in the figures shown below.

2.2 Lentiviral vector production

To produce lentiviral vectors expressing green fluorescent protein (GFP), HEK293 cells were plated in a 100 mm culture dish at a density of 3 750 000 cells in Dulbecco's modified eagle medium (DMEM; Sigma-Aldrich, Diegem, Belgium) with 10% fetal calf serum (FCS) and without penicillin/streptomycin (P/S). After 24 h, the culture medium was replaced by X-VIVO 15 medium (Lonza, Verviers, Belgium) without FCS and P/S. Cells were co-transfected by adding plasmids (2.75 µg pCMV-VSVG, 6.875 µg pRRL-CMV-GFP, 5.5 µg pMDLG-pRRE and 2.75 µg pRSV-REV) and FuGENE HD Transfection Reagent (Promega, Leiden, The Netherlands) at a 3:1 ratio of FuGENE HD Transfection Reagent to total DNA. All plasmids were kindly provided by dr. R.C. Hoeben (University Medical Center, Leiden, The Netherlands). HEK293 cells were incubated at 37 °C in a humidified incubator with a 5% CO_2 atmosphere for production of GFP-expressing lentiviral vectors under control of the eukaryotic promotor pRRL-CMV-GFP. After 48 h, lentiviral supernatant was harvested and stored at –80 °C until CASCs transduction.

2.3 CASCs isolation and expansion

Female Sprague-Dawley rats (n = 72, weight = 100 – 125 g) were used for CASCs isolation. Animals were sacrificed by an intraperitoneal injection with an overdose of Doléthal (200 mg/kg, Vétoquinol, Aartselaar, Belgium). The hearts were harvested, perfused with a normal Tyrode solution (137 mM NaCl, 5.4 mM KCl, 0.5 mM MgCl2, 1 mM CaCl2, 11.8 mM Na-HEPES, 10 mM glucose, 20 mM taurine, pH 7.4) and the right atrial appendage was removed. The extracted right atrial appendage tissue was minced in pieces of ~1 mm^3, washed with phosphate-buffered saline (PBS) and enzymatically dissociated for 30 min in Hank's Balanced Salt Solution (HBSS) containing 0.6 WU/ml collagenase NB 4 (Serva, Heidelberg, Germany) and 20 mM $CaCl_2$. Next, $ALDH^+$ cells were stained according to the Aldefluor kit (STEMCELL Technologies, Grenoble, France). In brief, the cell suspension was centrifuged at 1200 rpm for 5 min and the cell pellet was resuspended in sterile Aldefluor Assay Buffer. The Aldefluor Reagent was added (1:200 ratio of Aldefluor Reagent to Aldefluor Assay Buffer) and cells were incubated at 37 °C for 45 min. As a negative control, a part of the cell mixture containing Aldefluor Reagent was immediately added to the ALDH inhibitor diethylaminobenzaldehyde (DEAB) in a 200:1 ratio. After incubation, cells were centrifuged and resuspended in Aldefluor Assay Buffer for cell sorting. $ALDH^+$ cells were defined as CASCs and were flow-sorted in X-VIVO 15 medium supplemented with 20% FCS and 2% P/S. Isolated CASCs were seeded in 6-well plates at a density of 60 000 cells/well in the same culture medium and incubated at 37 °C in a humidified incubator with a 5% CO_2 atmosphere. At passage 1 (P1), cells were cultured at a density of 60 000 cells/well in X-VIVO 15 medium containing 10% FCS and 2% P/S. Cells were allowed to adhere and 24 h later, CASCs were transduced with a GFP-expressing lentiviral vector under control of the eukaryotic promotor pRRL-CMV-GFP. In brief, lentiviral supernatant of HEK293 cells was diluted 1:2 in X-VIVO 15 medium containing 10% FCS and 16 µg/ml polybrene and added to CASCs. Cells were incubated for 5 h at 37 °C and 5% CO_2, after which fresh X-VIVO 15 culture medium with 10% FCS and 2% P/S was added to the cells. After 1 week of incubation, CASCs were harvested, centrifuged for 5 min at 1200 rpm and resuspended at a density of $2.5x10^6 \pm 1x10^6$ cells in a Matrigel construct containing 44.4% X-VIVO 15 medium supplemented with 10% FCS, 2% P/S, 2% Amphotericin B, 34% collagen type I, 16% Matrigel and 1.7% sodium bicarbonate ($NaHCO_3$). CASCs were kept on ice in a 29-gauge needle (Terumo Medical Corporation, Leuven, Belgium) until use for intramyocardial injections.

2.4 Induction of myocardial infarction

Chronic MI was performed in adult female Sprague-Dawley rats by permanent ligation of the left anterior descending (LAD) coronary artery. The overall mortality rate after LAD occlusion was 51%, resulting in 36 surviving animals. In brief, rats were anesthetized using 2% isoflurane supplemented with oxygen, intubated via a transversal incision in the trachea and mechanically ventilated. A left thoracotomy was performed in the intercostal space between the third and fourth rib to expose the heart. The pericardium was opened, the thymus was partially removed and the LAD coronary artery was occluded with 6/0 Prolene suture (Ethicon, Diegem, Belgium). Successful occlusion was confirmed by LV pallor immediately after ligation. Rats undergoing MI received either no injections (MI animals, n = 11) or intramyocardial injections containing $2.5x10^6 \pm 1x10^6$ cells (MI + CASCs animals, n = 14). Intramyocardial injections were performed with a maximal total volume of 150 µl at three different points around the peri-infarct zone. The chest was closed and the lungs were re-inflated. After restoration of spontaneous respiration, the animal was extubated and the trachea was closed. SHAM animals (n = 11) underwent the same surgical procedure without LAD ligation and without injections. Methacam (1 mg/kg, Boehringer, Germany) was administered subcutaneously postoperatively once a day for two consecutive days. Rats with signs of redness and swelling around wounds were administered with antibiotics (10 mg/kg/day, Baytril, Bayer, Belgium) via the drinking water.

2.5 Evaluation of *in vivo* cardiac function

2.5.1 Conventional echocardiography

Transthoracic echocardiographic images were obtained from all animals under 2% isoflurane anesthesia supplemented with oxygen at baseline and 4 weeks postoperative with a Vivid *i* ultrasound machine (GE Vingmed Ultrasound, Horten, Norway) and a 10 MHz array transducer. Parasternal long axis and short axis views at mid-ventricular level were acquired in B-mode. From parasternal long axis images, LV end-diastolic diameter (LVEDD) and LV end-systolic diameter (LVESD) were obtained. In parasternal short axis views, anterior wall thickness (AWT), posterior wall thickness (PWT), LV inner diastolic diameter (LVIDD) and LV inner systolic diameter (LVISD) were determined. Heart rate (HR) was obtained from parasternal short axis views at mid-ventricular level in M-mode. End-diastolic volume (EDV) and end-systolic volume (ESV) were determined by the formula $(\pi * LVIDD^2 * LVEDD)/6$ and $(\pi * LVISD^2 * LVESD)/6$ respectively. Subsequently, stroke volume (SV) was calculated as EDV-ESV and cardiac output (CO) was measured as (SV*HR)/1000. Finally, ejection fraction (EF) was obtained by (EDV-ESV)/EDV and is expressed in %.

2.5.2 Hemodynamic measurements

Invasive hemodynamic measurements were obtained at sacrifice from all animals under 2% isoflurane anesthesia supplemented with oxygen. LV pressures were measured with an SPR-320 Mikro-Tip single pressure catheter (Millar Inc., Houston, USA) that was moved into the LV via the right carotid artery. The catheter was connected to a quad-bridge amplifier and PowerLab26T module (AD Instruments, Oxford, United Kingdom) to transfer the pressure data to LabChart v7.3.7 software (AD Instruments, United Kingdom). Hemodynamic parameters (*i.e.* maximum LV pressure, minimum LV pressure, end-diastolic pressure (EDP), mean pressure, peak rate of pressure rise (dP/dt_{max}), peak rate of pressure decline (dP/dt_{min}) and relaxation time constant (Tau)) were obtained from this software.

2.6 Cardiomyocyte isolation and unloaded cell shortening

Four weeks after surgery, rats were sacrificed by an intraperitoneal injection with an overdose of Doléthal (200 mg/kg). The hearts were harvested and single cardiomyocytes were isolated from the LV by enzymatic dissociation through retrograde perfusion of the aorta. The hearts were perfused for 1 min with a normal Tyrode solution and then connected to a Langendorff perfusion system for following perfusion steps at 37 °C and 100% O_2 oxygenation. Perfusion with a Ca^{2+} -free solution (130 mM NaCl, 5.4 mM KCl, 1.2 mM KH_2PO_4, 1.2 mM $MgSO_4$, 6 mM HEPES, 20 mM glucose, pH 7.2) was performed for 8 min, followed by perfusion with an enzyme solution (Ca^{2+} -free solution containing 1.5 g/l collagenase type II (Worthington, Lakewood, USA) and 0.06 g/l protease type XIV (Sigma-Aldrich, Diegem, Belgium)) for variable time periods (12 – 20 min). Finally, hearts were perfused with a low Ca^{2+} solution (Ca^{2+} -free solution containing 0.1 mM $CaCl_2$ and 20 mM taurine) for 5 min. The digested LV tissue was minced and filtered, after which Ca^{2+} concentration was gradually increased to 1 mM with normal Tyrode solution. Unloaded cell shortening experiments were performed on intact cardiomyocytes in normal Tyrode at room temperature. Cardiomyocyte shortening was measured with a video-edge detector (Crescent Electronics, USA) during field stimulation with constant pulses above threshold at 1, 2 and 4 Hz using platinum electrodes. Data were normalized to diastolic cell length and presented as fractional shortening (L/L_0, %). Kinetics of cell shortening were assessed by measuring time to peak contraction (TTP, ms) and time to half time relaxation (time to RT_{50}, ms).

2.7 Fibrosis measurement

Transversal frozen tissue sections of 10 µm were obtained from the LV and stained according to the Sirius Red/Fast Green Collagen Staining Kit for frozen sections (Chondrex Inc, Kampenhout, Belgium). After staining, sections were dehydrated in increasing concentrations of ethanol, followed by a xylene

wash and mounted in DPX mounting medium. From all animals, four randomly chosen images were obtained in the peri-infarct zone and LV remote region using a Leica DM2000 LED microscope (Leica Microsystems, Diegem, Belgium). Interstitial collagen was indicated by a red color and non-collagenous tissue by a green color. The percentage of collagen deposition was quantified with AxioVision 4.6 software (Carl Zeiss, Zaventem, Belgium). Blood vessels were excluded.

2.8 Immunohistochemistry

From frozen LVs, transversal tissue sections of 10 µm thick were obtained. Sections were washed 3 times in PBS and blocked for 1 h with 20% protein block (Dako, X0909, Heverlee, Belgium) and 0.1% PBS-Triton (PBS-T). Sections were incubated overnight at 4 °C with fluorescein isothiocyanate (FITC)-conjugated anti-GFP primary antibody (1:100, goat polyclonal, ab6662, Abcam, Cambridge, UK) in PBS containing 1% protein block and 0.1% PBS-T. After washing in PBS, sections were immersed once in 70% ethanol and 8 times in PBS, followed by staining with 4',6-diamidino-2-phenylindole (DAPI) before mounting. Images were acquired using a Leica DM4000 B LED microscope (Leica Microsystems, Diegem, Belgium).

2.9 Propidium iodide assay

CASCs (P1) were seeded in 96-well plates at a density of 10 000 cells/well in Minimal essential medium, alpha modification (α-MEM, Sigma-Aldrich, Diegem, Belgium) supplemented with 10% FCS, 1% P/S and 1% L-glutamine (Sigma-Aldrich, Diegem, Belgium) and cells were allowed to adhere for 24 h. To assess the effect of DPSCs on CASCs proliferation, CASCs were incubated with conditioned medium (CM) of DPSCs (kindly provided by the lab of prof. Bronckaers) in presence of 2% FCS for 24 h. To investigate whether DPSCs affect CASCs viability, CASCs were incubated with serum-free CM of DPSCs for 48 h. After incubation steps, CM of DPSCs was replaced by Lysis buffer A100 (ChemoMetec, Allerod, Denmark), followed by adding an equal amount of Lysis buffer B (ChemoMetec, Allerod, Denmark) containing 10 µg/ml propidium iodide (PI) solution (Sigma-Aldrich, P4864, Diegem, Belgium). CASCs were incubated for 15 min at room temperature, after which the fluorescence intensity was measured at excitation wavelength of 540 nm and emission wavelength of 612 nm using the FLUOstar OPTIMA Microplate Reader (BMG Labtech, Germany). For both proliferation and viability assays, CASCs were incubated with α-MEM supplemented with 10% FCS, 1% P/S and 1% L-glutamine as positive control. As negative control, CASCs were incubated with α-MEM supplemented with 1% P/S, 1% L-glutamine and 2% FCS for proliferation assays or serum-free for viability assays.

2.10 Transwell migration assay

CASCs (P1) were seeded at a density of 100 000 cells into culture inserts with porous membrane of 8 µm pore size (ThinCert, Greiner Bio-One, Vilvoorde, Belgium). Inserts were placed onto 24-well plates containing CM of DPSCs at the bottom. α-MEM with 1% P/S, 1% L-glutamine and 10% FCS was used as positive control and serum-free α-MEM with 1% P/S and 1% L-glutamine as negative control. After 24 h of migration, the wells and inserts were washed with PBS and fixed with 4% PFA for 15 min, followed by staining with 0.1% crystal violet for 30 min. Cells that did not migrate were removed at the top side of the insert, after which the amount of transmigrated CASCs was quantified with AxioVision 4.6 software (Carl Zeiss, Zaventem, Belgium).

2.11 Reverse transcriptase PCR

Total RNA was extracted from CASCs (P1) according to the RNeasy fibrous tissue kit (Qiagen, Antwerpen, Belgium) with the exception that cells were lysed with QIAzol (Qiagen, Antwerpen, Belgium) and RNA was extracted using chloroform. In addition, proteinase K and DNase I digestion steps were not performed. Quantity and purity of extracted RNA were determined using the NanoDrop 2000 spectrophotometer (Isogen Life Science, Temse, Belgium). cDNA was synthesized using qScript cDNA SuperMix (QuantaBio, 95048, Leuven, Belgium) and reverse transcriptase polymerase chain reaction (RT-PCR) was performed using the T100 Thermal Cycler (Bio-Rad, Temse, Belgium). Primers for vascular endothelial growth factor receptor 1 (VEGFR1) which span an exon-exon junction were designed in *Rattus norvegicus*. Primers used for RT-PCR are summarized in Table 1. Glyceraldehyde 3-phosphate dehydrogenase (GAPDH) was used as reference gene. PCR-products were loaded on a 1.5% agarose gel stained with gelred and visualized under UV light.

Table 1: VEGFR1 primer sequences for RT-PCR.

VEGFR1 transcript variant	**Primer sequences (5' – 3')**	
	Forward primer	Reverse primer
Transcript variant 1	CAGAAGGGGGTCGTGGAAAG	CGGAAGAAGACCGCTTCAGTT
Transcript variant 2	TTACGTCACAGATGTGCCAA	GCAGTGCTCACCTCTAACGA
All transcript variants	TTTCTCAAGTGCAGAGGGGAG	GTCAGGGGTAAGAGCGTCAA
GAPDH	ACCACAGTCCATGCCATCAC	TCCACCACCCTGTTGCTGTA

VEGFR1, vascular endothelial growth factor receptor 1; RT-PCR, reverse transcriptase polymerase chain reaction; GAPDH, glyceraldehyde 3-phosphate dehydrogenase.

2.12 Statistics

Statistical analyses were performed using GraphPad Prism 8.1.1 software. Normal distribution of data was assessed with D'Agostino & Pearson test. For echocardiographic, hemodynamic and unloaded cell shortening experiments, One-way Anova with Bonferroni's multiple comparisons test was performed if data were normally distributed. If data were not normally distributed, Kruskal Wallis with Dunn's multiple comparisons test was used. Proliferation and viability assays were analyzed using Mann-Whitney U test. For migration assays, Wilcoxon singed rank test was performed. All data are expressed as mean ± standard error of the mean (SEM). A value of $p < 0.05$ was considered statistically significant.

3 Results

3.1 CASCs transplantation improves echocardiographic and hemodynamic parameters after MI

In vivo cardiac function was assessed by echocardiographic and hemodynamic measurements. Echocardiographic data of SHAM, MI and MI + CASCs animals 4 weeks postoperative are summarized in Table 2. All echocardiographic parameters remained unchanged after induction of chronic MI (Figure 3A-H). CASCs transplantation significantly increased EF (Figure 3B; p = 0.0166) and AWT (Figure 3C; p = 0.0482). In addition, CASCs therapy significantly reduced ESV (Figure 3F; p = 0.0108) compared to MI. Other echocardiographic parameters remained unchanged after CASCs transplantation.

Table 2: Conventional echocardiographic characteristics.

Parameters	**4 weeks postoperative**		
	SHAM (n = 4)	MI (n = 11)	MI + CASCs (n = 4)
HR (bpm)	332 ± 23	328 ± 13	360 ± 15
EF (%)	70 ± 4	60 ± 5	86 ± 3 *
AWT (mm)	1.11 ± 0.13	1.06 ± 0.09	1.47 ± 0.06 *
PWT (mm)	1.51 ± 0.1	1.36 ± 0.09	1.67 ± 0.07
EDV (µl)	206 ± 16	256 ± 21	187 ± 21
ESV (µl)	60 ± 6	107 ± 20	26 ± 7 *
SV (µl)	147 ± 18	149 ± 12	161 ± 20
CO (ml/min)	48 ± 4	50 ± 5	59 ± 9

HR, heart rate; EF, ejection fraction; AWT, anterior wall thickness; PWT, posterior wall thickness; EDV, end-diastolic volume; ESV, end-systolic volume; SV, stroke volume; CO, cardiac output. Data are expressed as mean ± SEM. * denotes p <0.05 *vs* MI.

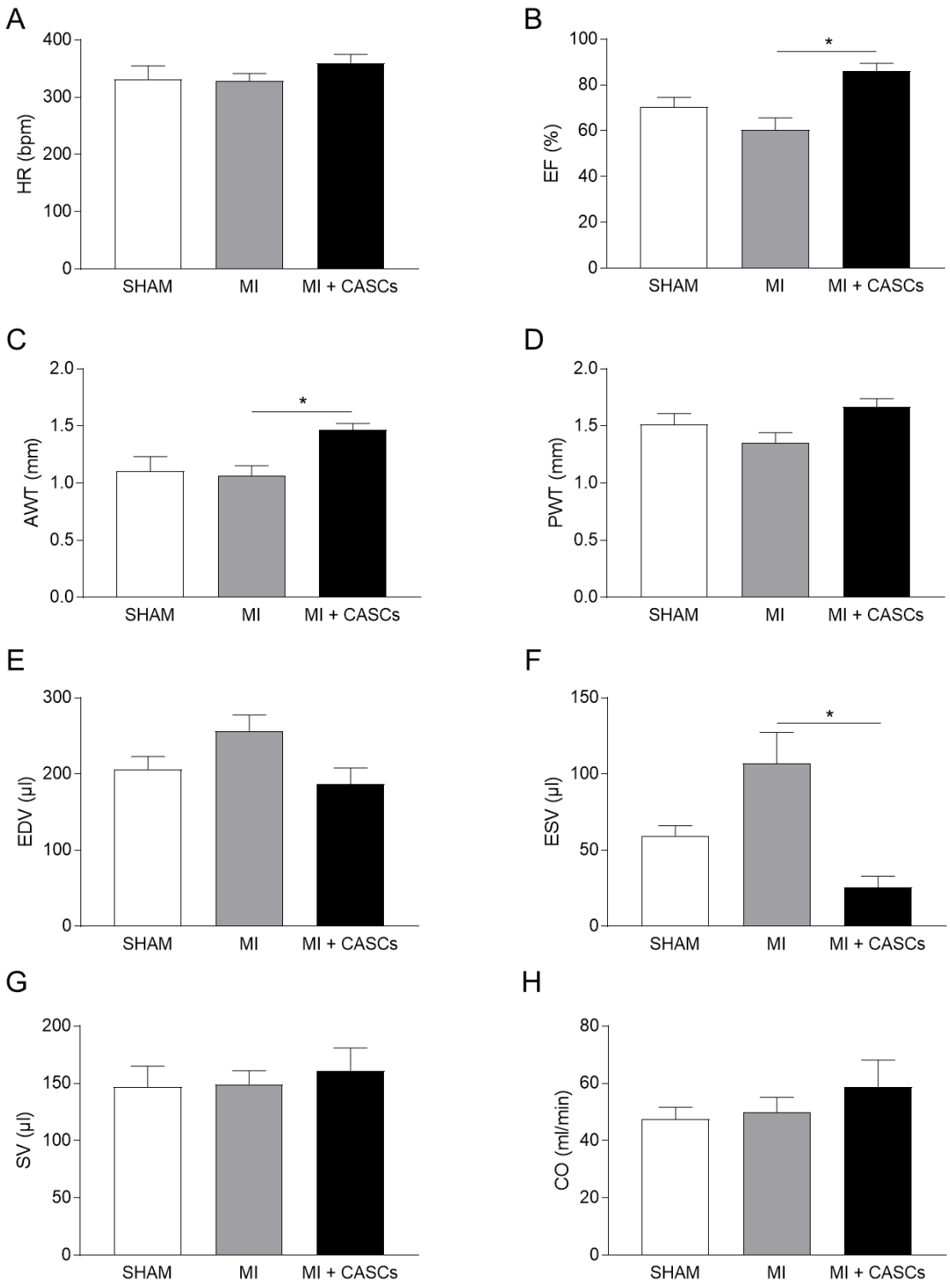

Figure 3: Echocardiographic parameters 4 weeks after surgery. Quantification of echocardiographic measurements in SHAM (n = 4), MI (n = 11) and MI + CASCs (n = 4) animals. Analyzed echocardiographic parameters are: (A) heart rate (HR), (B) ejection fraction (EF), (C) anterior wall thickness (AWT), (D) posterior wall thickness (PWT), (E) end-diastolic volume (EDV), (F) end-systolic volume (ESV), (G) stroke volume (SV) and (H) cardiac output (CO). Data are expressed as mean ± SEM. * denotes $p < 0.05$.

All data of hemodynamic measurements of SHAM, MI and MI + CASCs animals 4 weeks after surgery are summarized in Table 3. Induction of chronic MI significantly increased mean LV pressure (Figure 4A; p = 0.0014), which was decreased again by transplantation of CASCs after MI (p = 0.0003). Maximum LV pressure did not differ after MI and remained unchanged after CASCs transplantation (Figure 4B). In contrast, minimum LV pressure and EDP were significantly increased after induction of MI (Figure 4C and D; p-values were respectively 0.0066 and 0.0129). CASCs transplantation significantly decreased minimum LV pressure and EDP compared to MI (p-values were respectively <0.0001 and 0.0001). Induction of MI did not change dP/dt_{max}, a measure of ventricular contractility (Figure 4E), and dP/dt_{min}, a measure of ventricular relaxation (Figure 4F). However, CASCs transplantation significantly increased dP/dt_{max} compared to MI (p = 0.0021), but did not change dP/dt_{min}. Finally, Tau was significantly increased after MI (Figure 4G; p = 0.0037), but remained unchanged after CASCs transplantation.

Table 3: Hemodynamic characteristics.

Parameters	**4 weeks postoperative**		
	SHAM (n = 10)	MI (n = 12)	MI + CASCs (n = 12)
Mean pressure (mmHg)	33 ± 2 **	45 ± 2	32 ± 2 ***
Max pressure (mmHg)	93 ± 3	97 ± 2	95 ± 3
Min pressure (mmHg)	-11.3 ± 4 **	2.9 ± 2	-18.9 ± 2.9 ****
EDP (mmHg)	-3.3 ± 3.2 *	9.6 ± 2.3	-9.6 ± 3.2 ***
dP/dt_{max} (mmHg/s)	7456 ± 549	6224 ± 234	9001 ± 704 ***
dP/dt_{min} (mmHg/s)	-8545 ± 834	-7300 ± 560	-8516 ± 553
Tau (s)	0.011 ± 0.001 **	0.014 ± 0.001	0.012 ± 0.001

Mean pressure, mean left ventricular pressure; max pressure, maximum left ventricular pressure; min pressure, minimal left ventricular pressure; EDP, end-diastolic pressure; dP/dt_{max}, peak rate of pressure rise; dP/dt_{min}, peak rate of pressure decline; Tau, relaxation time constant. Data are expressed as mean ± SEM. * denotes p <0.05, ** denotes p <0.01, *** denotes p <0.001 and **** denotes p <0.0001 *vs* MI.

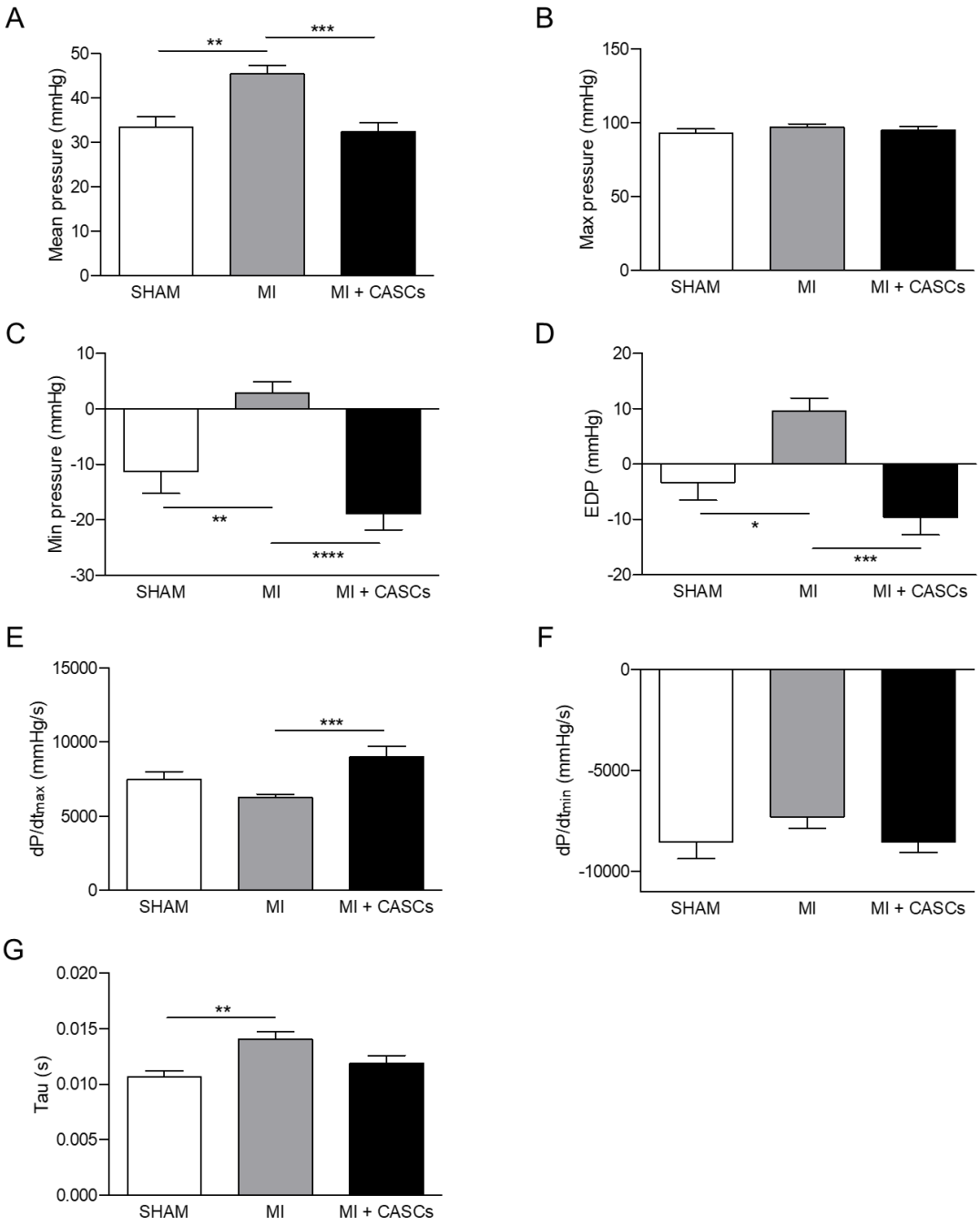

Figure 4: Hemodynamic parameters 4 weeks after surgery. Quantification of hemodynamic measurements in SHAM (n = 10), MI (n = 12) and MI + CASCs (n = 12) animals. Measurement of hemodynamic parameters: (A) mean left ventricular pressure, (B) maximum left ventricular pressure, (C) minimum left ventricular pressure, (D) end-diastolic pressure (EDP), (E) peak rate of pressure rise (dP/dt_{max}), (F) peak rate of pressure decline (dP/dt_{min}) and (G) relaxation time constant (Tau). Data are expressed as mean ± SEM. * denotes $p < 0.05$, ** denotes $p < 0.01$, *** denotes $p < 0.001$ and **** denotes $p < 0.0001$.

3.2 CASCs transplantation restores resident cardiomyocyte shortening and kinetics

Because no CASCs could be identified after single cardiomyocyte isolation, unloaded cell shortening experiments were only performed on resident cardiomyocytes. Figure 5A is a representative example of unloaded cell shortening during field stimulation at 1, 2 and 4 Hz in resident cardiomyocytes isolated from SHAM, MI and MI + CASCs animals 4 weeks after surgery. Induction of chronic MI significantly decreased fractional shortening at 4 Hz compared to SHAM (Figure 5B, right panel; $p = 0.0008$), but did not change cell shortening at 1 and 2 Hz (Figure 5B, left and middle panel). Resident cardiomyocyte shortening at 4 Hz was significantly increased after CASCs transplantation ($p = 0.0052$), but remained unchanged at 1 and 2 Hz. Both time to peak of contraction and time to half-relaxation, represented as TTP and time to RT_{50} respectively, of resident cardiomyocytes were significantly increased at 1, 2 and 4 Hz after MI (Figure 5C and D; p-values were all <0.05). CASCs transplantation significantly decreased TTP and time to RT_{50} at 1, 2 and 4 Hz compared to MI (p-values were all <0.01).

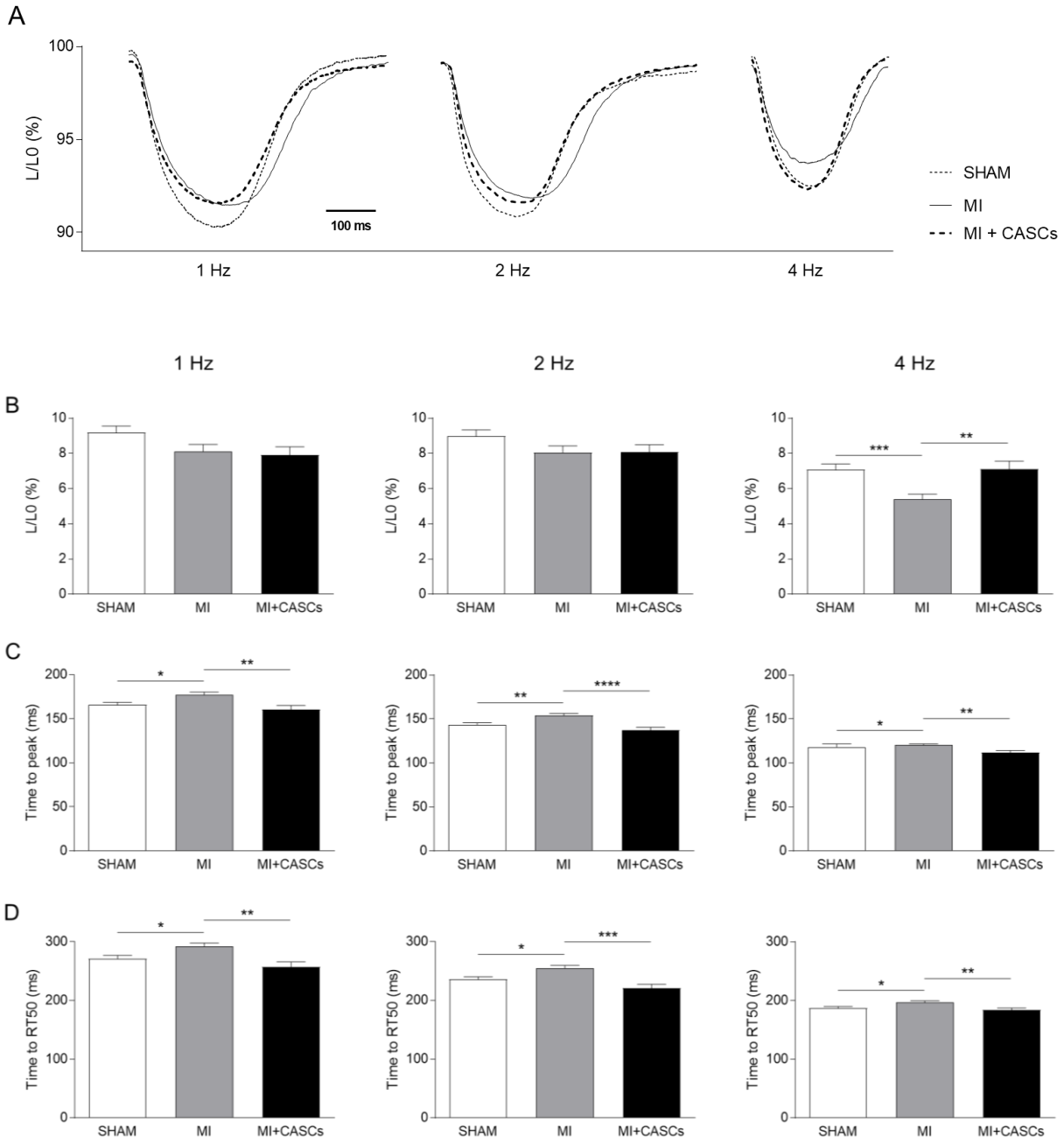

Figure 5: Resident cardiomyocyte shortening during field stimulation at 1, 2 and 4 Hz. (A) Representative example of fractional cell shortening (L/L0) at 1, 2 and 4 Hz in resident cardiomyocytes from SHAM (n_{cells} 1 Hz = 88, n_{cells} 2 Hz = 86, n_{cells} 4 Hz = 80), MI (n_{cells} 1 and 2 Hz = 72, n_{cells} 4 Hz = 60) and MI + CASCs animals (n_{cells} = 41). Scale bar = 100 ms. (B) Resident cardiomyocyte shortening (L/L0), (C) time to peak and (D) time to half-relaxation during field stimulation at 1, 2 and 4 Hz from SHAM, MI and MI + CASCs animals. Data are expressed as mean ± SEM. * denotes p <0.05, ** denotes p <0.01, *** denotes p <0.001 and **** denotes p <0.0001.

Figure 6 shows the effect of CASCs transplantation on resident cardiomyocyte L/L0 in a frequency-dependent way, since the significant improvement in cell shortening was only observed at 4 Hz. CASCs transplantation showed a significant effect at all frequencies for TTP and time to RT_{50}, indicating that the effect of CASCs transplantation was not frequency-dependent for resident cardiomyocyte kinetics.

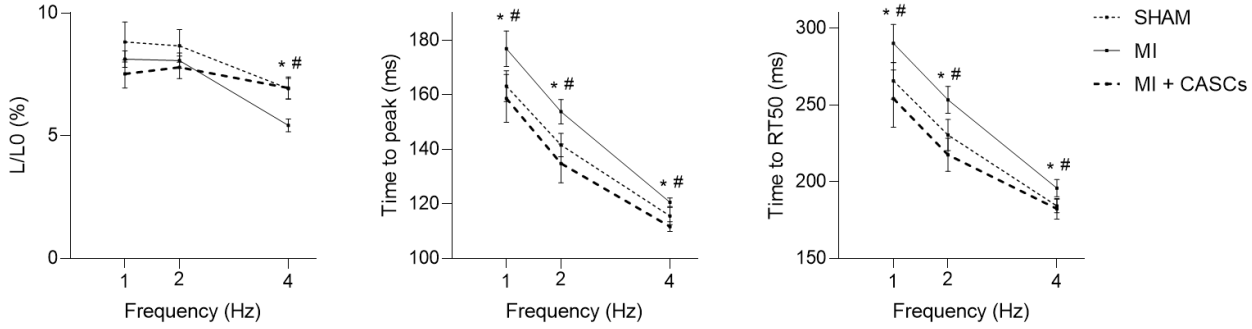

Figure 6: Frequency dependence of resident cardiomyocyte shortening during field stimulation at 1, 2 and 4 Hz. Frequency dependence of fractional cell shortening (L/L0, left), time to peak (TTP, middle) and time to half-relaxation (time to TP50, right) in resident cardiomyocytes from SHAM (n_{cells} 1 Hz = 88, n_{cells} 2 Hz = 86, n_{cells} 4 Hz = 80), MI (n_{cells} 1 and 2 Hz = 72, n_{cells} 4 Hz = 60) and MI + CASCs animals (n_{cells} = 41). * denotes $p < 0.05$ for SHAM *vs* MI. # denotes $p < 0.05$ for MI + CASCs *vs* MI.

3.3 Interstitial collagen deposition tends to decrease after CASCs transplantation

Figure 7A is a representative example of hearts from SHAM, MI and MI + CASCs animals 4 weeks after surgery. Representative images of interstitial collagen obtained by Sirius Red/Fast Green staining in LV sections from SHAM, MI and MI + CASCs animals are provided in Figure 7B. As summarized in Figure 7C, interstitial collagen deposition tended to increase after induction of MI. In addition, CASCs transplantation tended to decrease LV collagen deposition. No statistical test was performed due to the limited sample size in the SHAM group.

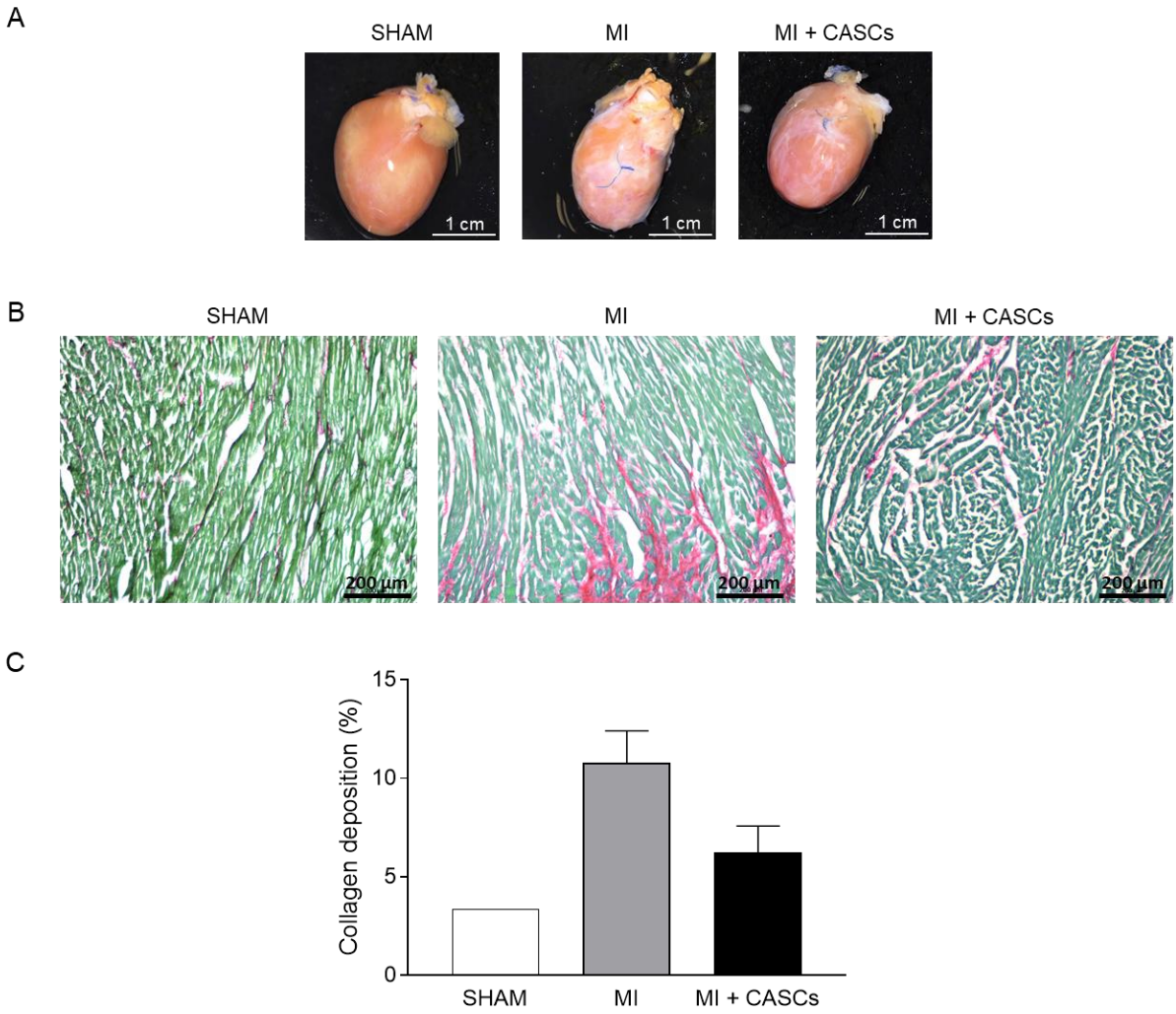

Figure 7: Interstitial collagen deposition in the LV. (A) Representative example of hearts from SHAM, MI and MI + CASCs animals. Scale bar = 1 cm. (B) Representative example of interstitial collagen (red) in the LV from SHAM, MI and MI + CASCs animals. The green color indicates non-collagenous proteins. Scale bar = 200 µm. (C) Percentage of total LV collagen deposition in the peri-infarct zone and LV remote region from SHAM (n = 1), MI (n = 6) and MI + CASCs (n = 5) animals. Data are expressed as mean ± SEM.

3.4 CASCs could not be identified in cardiac tissue

Engraftment of CASCs in cardiac tissue 4 weeks after surgery was assessed by immunohistochemical staining for GFP-labeled CASCs (Figure 8). No CASCs engraftment was observed in LV transversal sections from MI + CASCs animals. However, resident cardiomyocytes showed a high degree of autofluorescence. Merged images showed no co-localization of nuclei with bright green dots, suggesting that these bright green fluorescent signals are derived from antibody aggregates, as indicated by white arrows.

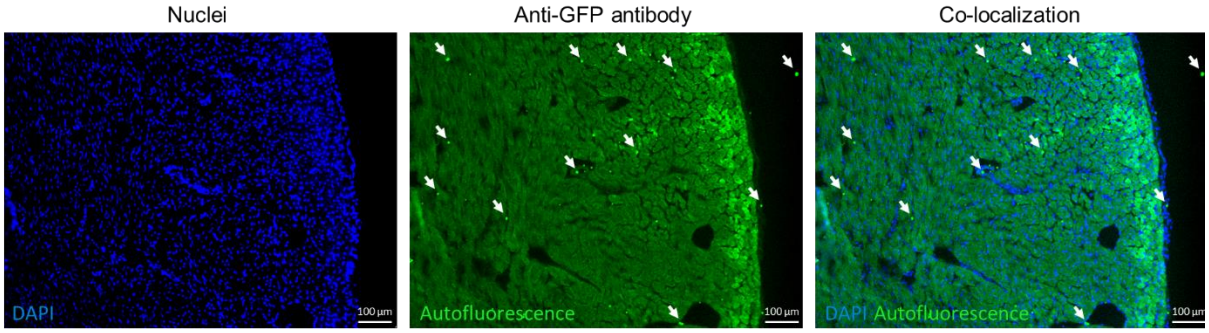

Figure 8: Immunohistochemical staining for GFP-CASCs. Representative example of anti-GFP staining to assess CASCs engraftment in cardiac tissue. Cell nuclei were stained with DAPI (blue). Autofluorescence of resident cardiac tissue is shown in green. Arrows indicate antibody aggregates. Scale bar = 100 µm. DAPI, 4',6-diamidino-2-phenylindole; GFP, green fluorescent protein; CASCs, cardiac atrial appendage stem cells.

3.5 Conditioned medium of DPSCs promotes CASCs proliferation and survival

The effect of DPSCs on CASCs proliferation and viability is shown in Figure 9. All data were normalized to negative control (= 100%). Positive controls of proliferation as well as viability propidium iodide assays showed significantly more CASCs proliferation and survival compared to negative control CASCs (p-values were respectively 0.0002 and 0.0004), indicating that both assays were correctly performed. CASCs incubated with CM of DPSCs proliferated significantly more compared to negative control (Figure 9A; p = 0.0005). Furthermore, CM of DPSCs induced significantly more survival of CASCs compared to negative control (Figure 9B; p = 0.0101).

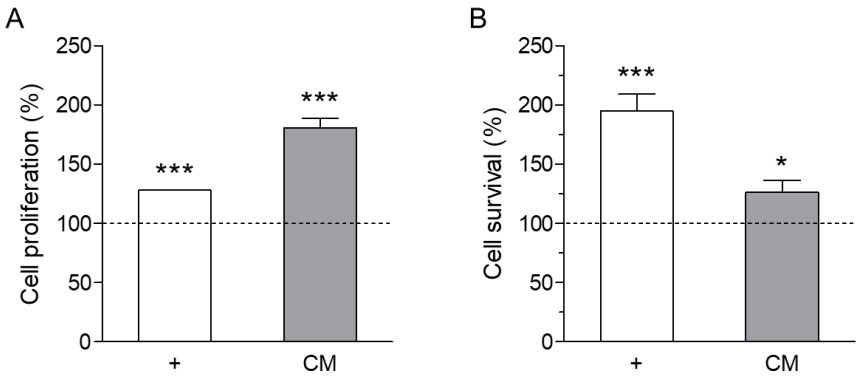

Figure 9: Effect of conditioned medium from DPSCs on CASCs proliferation and survival. Quantification of propidium iodide assay for (A) proliferation (assay was performed 1 time) and (B) viability (assay was performed 2 times) in positive control (+, n=1 for proliferation, n=2 for viability) and conditioned medium from DPSCs (CM, n=7). Values were normalized to negative control (= 100%). Data are expressed as mean ± SEM. * denotes p <0.05 and *** denotes p <0.001 *vs* negative control.

3.6 Conditioned medium of DPSCs promotes CASCs migration

A representative example of CASCs migration towards negative control medium (left panel) and CM of DPSCs (right panel) is provided in Figure 10A. CM of DPSCs significantly increased CASCs migration compared to negative control (Figure 10B; p = 0.0313).

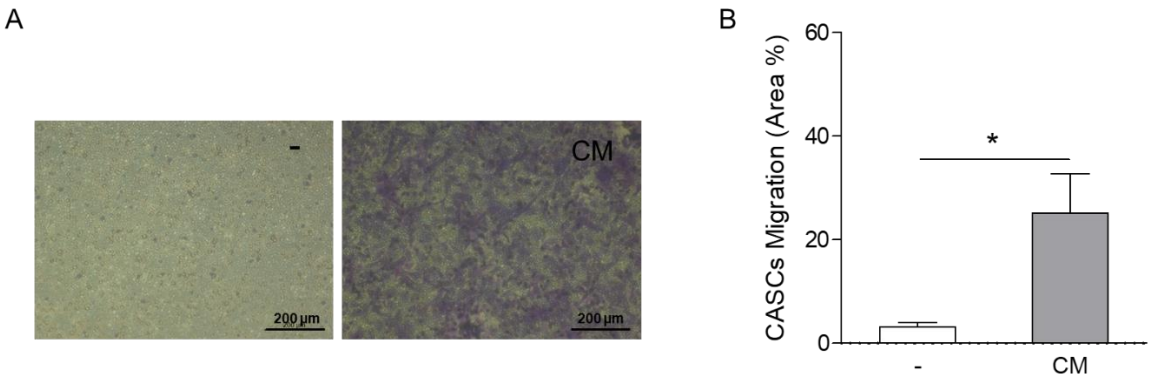

Figure 10: Effect of conditioned medium from DPSCs on CASCs migration. (A) Representative example of CASCs migration towards negative control (-) and conditioned medium (CM). Scale bar = 200 µm. (B) Quantification of transwell migration assay from negative control (-, n=6) and conditioned medium (CM, n=6). Data are expressed as mean ± SEM. * denotes p <0.05 *vs* negative control.

3.7 CASCs genetically express VEGFR1

To elucidate one of the mechanisms by which DPSCs can boost CASCs properties, RT-PCR was performed on CASCs mRNA to investigate whether CASCs express the VEGFR1 gene. mRNA was isolated from 6 CASCs samples. Primers specific for VEGFR1 transcript variant 1, VEGFR1 transcript variant 2 and unspecific for VEGFR1 transcript variants were used. GAPDH was used as reference gene. All 6 CASCs samples showed gene expression of VEGFR1 and specifically transcript variants 1 and 2 (Figure 11).

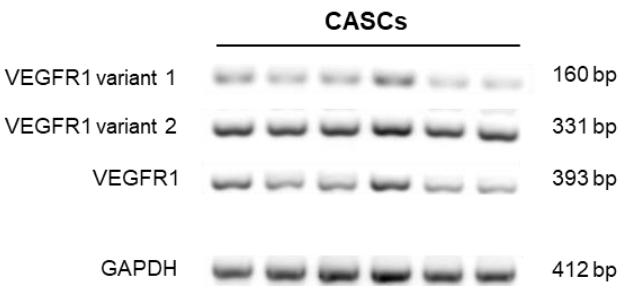

Figure 11: Gene expression of VEGFR1 by CASCs. Representative RT-PCR of VEGFR1 and specifically VEGFR1 transcript variants 1 and 2 from 6 CASCs samples. GAPDH was used as reference gene. VEGFR1, vascular endothelial growth factor receptor 1; CASCs, cardiac atrial appendage stem cells; GAPDH, glyceraldehyde 3-phosphate dehydrogenase.

4 Discussion

In this study, we demonstrate that induction of chronic MI leads to *in vivo* cardiac diastolic dysfunction and functional remodeling in resident cardiomyocytes. CASCs transplantation is able to improve cardiac function both at the organ and cellular level, showing the efficacy of CASCs therapy in MI. However, no CASCs were identified in cardiac tissue. In addition, we demonstrate that DPSCs can boost CASCs functional properties, focusing on proliferation, viability and migration.

4.1 CASCs transplantation improves *in vivo* cardiac function after MI

In vivo cardiac function was assessed in SHAM, MI and MI + CASCs animals 4 weeks postoperative by echocardiographic and hemodynamic measurements. Our data showed no significant changes in echocardiographic parameters after induction of chronic MI compared to SHAM operated animals, thereby indicating that global cardiac function and LV morphology were not altered in MI. However, it is possible that significance was not reached for echocardiographic measurements due to the low sample size in SHAM and MI animals. Therefore, sample size will be increased in a future study to assure that reliable conclusions are drawn. In contrast with our results, a previous study in our laboratory showed a significant reduction in EF, AWT and PWT in MI animals associated with increased EDV and ESV, which is all typical for animals with a large MI (64). When sample size will be increased, we also expect that these parameters will be altered in the MI group compared to SHAM.

As observed by hemodynamic measurements, induction of MI tended to reduce dP/dt_{max} compared to SHAM animals, but data were not significant. In addition, maximum LV pressure remained unchanged, indicating only limited systolic dysfunction after MI observed by hemodynamic measurements. Importantly, MI significantly increased minimum LV pressure, EDP and Tau, and tended to increase dP/dt_{min}. These are all parameters for cardiac diastolic function. As such, our hemodynamic data show a larger LV diastolic dysfunction than systolic dysfunction in MI animals compared to SHAM. The same results were observed in a previous study performed in our laboratory (64).

Nevertheless, studies have shown that immediately after coronary artery occlusion, cardiomyocyte cell death results in the abrupt reduction of CO (65, 66). As a consequence of the loss of functional contractile muscle mass, compensatory mechanisms are activated to preserve sufficient perfusion of vital organs. First, acute and beneficial compensatory adaptations are initiated after MI to maintain hemodynamic homeostasis. These adaptations include activation of the Frank-Starling mechanism, an intrinsic response of the heart to a reduction in CO, and hyperactivation of neurohormonal pathways. Our study showed that MI is associated with an increase in minimal LV and end-diastolic pressures

without changes in maximal LV pressure, CO and SV. In MI, LV contractile function is typically impaired leading to incomplete LV emptying. Consequently, blood accumulates in the LV during diastole, thereby increasing EDV and EDP. This is in accordance with the Frank-Starling principle, which explains that a greater EDP (*i.e.* higher preload) increases sarcomere tension, making the heart able to generate more systolic pressure and to deliver more blood to the organs. As such, this may be a mechanism by which maximal LV pressure, CO and SV were maintained within normal values in MI animals in our study. Another reason for the unchanged maximal LV pressure, CO an SV in MI animals compared to SHAM could be the neurohormonal activation of the SNS and RAAS, which enhances cardiac contractility and peripheral resistance (66). In short-term, compensatory mechanisms are therefore beneficial. Although, chronic activation of these mechanisms is detrimental because it causes adverse ventricular remodeling followed by ventricular dilatation, eventually leading to the development of heart failure (13).

Our study demonstrated that CASCs transplantation partially improved *in vivo* cardiac function by increasing EF and AWT and by decreasing ESV. Other echocardiographic parameters, such as SV and CO, tended to increase. However, it is possible that significance was not reached for these parameters due to the low sample size in MI and MI + CASCs animals. When sample size will be increased in a future study, it is expected that SV, CO and PWT will also be significantly increased, and that EDV will be significantly decreased compared to MI. Furthermore, CASCs transplantation was able to restore several LV pressure parameters after MI. Mean LV pressure, minimum LV pressure and EDP were normalized to SHAM values after CASCs transplantation. Although only a trend was observed in dP/dt_{min} and Tau, CASCs therapy was able to improve cardiac diastolic function. In addition, dP/dt_{max} was significantly increased after CASCs transplantation compared to MI without treatment, but no changes were observed in maximum LV pressure. Nevertheless, this indicates an improvement in cardiac systolic function in animals injected with CASCs after MI. A previous study investigating the therapeutic effect of CASCs in a mini-pig model showed that CASCs could preserve cardiac function after MI by increasing EF and by preserving regional wall thickening in mid-ventricular and mid-anteroseptal segments (56). However, CASCs therapy could not improve EDV and ESV 2 months after transplantation. Overall, this study showed that cardiac systolic and diastolic function in rats receiving CASCs therapy was improved compared to MI animals. This indicates that CASCs could prevent or restore cardiac dysfunction after MI. There are several potential mechanisms by which CASCs could counteract adverse remodeling and induce cardiac repair after MI (67, 68). First, CASCs could be differentiated into functional cardiomyocytes, thereby replacing the lost cardiomyocytes in the infarcted area. In the study of Fanton *et al.*, we also showed that CASCs are able to express cardiac proteins after *in vivo* transplantation (56). Therefore, this is the most likely hypothesis. In addition,

paracrine factors secreted by transplanted CASCs could promote endogenous stem cell migration towards the site of injury, followed by proliferation and differentiation into ventricular cardiomyocytes, leading to myocardium regeneration. The second mechanism suggests that CASCs secrete paracrine factors to promote survival and proliferation of resident cardiomyocytes, thereby protecting them from adverse remodeling. In addition, it is possible that CASCs reduced inflammation and subsequent cardiac fibrosis via paracrine mechanisms, thereby preventing cardiac dysfunction. Finally, CASCs are able to induce angiogenesis. The formation of new blood vessels in the infarcted tissue is essential for cardiomyocyte recovery and limits infarct expansion. Therefore, revascularization is a third mechanism by which CASCs could improve cardiac function.

Because of the variable amount of CASCs obtained after *ex vivo* expansion, animals receiving CASCs transplantation could be divided into two groups depending on the concentration of cells that were intramyocardially injected: animals injected with $\pm 2x10^6$ CASCs and animals injected with $\pm 4x10^6$ CASCs. To assess whether CASCs concentration has an effect on the extent of cardiac repair, hemodynamic data of these two groups were compared. There was no significant difference in hemodynamic parameters between animals injected with $2x10^6$ and $4x10^6$ CASCs (data not shown). This indicates that CASCs concentration has no effect on cardiac repair. However, more experiments including echocardiographic measurements should be performed to confirm this conclusion. In a double-blind, placebo-controlled, dose-ranging study, patients with acute MI were intravenously infused with three different concentrations of human MSCs: either $0.5x10^6$, $1.6x10^6$ or $5x10^6$ cells/kg (69). Overall, cardiac function was improved when patients were treated with human MSCs compared to placebo. All analyzed parameters, except for premature ventricular contraction count, showed no dose-dependent effects of human MSC therapy, which is in line with our findings. Another dose comparison study performed transendocardial injection of $20x10^6$ or $100x10^6$ human MSCs in patients with ischemic cardiomyopathy (70). In this study, EF was significantly increased in the highest dose, but all other cardiac parameters remained unchanged between the two doses. It is possible that in our study the difference in concentration between $\pm 2x10^6$ and $\pm 4x10^6$ CASCs was not large enough to detect a dose-dependent effect. On the other hand, a concentration of $\pm 4x10^6$ cells could be too high for intramyocardial injection in rat hearts, indicating that no dose-dependent effect was observed because the stem cells were partially cleared from the cardiac tissue (59). Furthermore, it is possible that significance was not reached between the two concentrations because the sample size in both groups was limited (n=7 for $\pm 2x10^6$ CASCs and n=5 for $\pm 4x10^6$ CASCs). Therefore, these experiments should be repeated in a larger sample population. Altogether, this study combined data of animals injected with $\pm 2x10^6$ and $\pm 4x10^6$ CASCs because no dose-dependent effect was observed.

4.2 CASCs transplantation improves resident cardiomyocyte contractility

Cardiac function was assessed on the cellular level by unloaded cell shortening experiments in resident cardiomyocytes from SHAM, MI and MI + CASCs animals. Induction of MI reduced resident cardiomyocyte shortening at 4 Hz and slowed down the contraction and relaxation kinetics at all frequencies. Although cell shortening after MI was reduced at 1 and 2 Hz compared to SHAM, data were not significant. This is in line with other studies investigating cardiomyocyte shortening after MI. In the article of Loennechen *et al.*, cell shortening was decreased at 2, 5, 7 and 10 Hz associated with prolonged TTP and time to RT_{50} 4 weeks after LAD ligation (71). In contrast, a previous study showed a reduced amplitude of cell shortening at 1, 2 and 4 Hz, but no changes in TTP contraction 8 weeks after permanent LAD ligation (72). CASCs transplantation after MI restored resident cardiomyocyte shortening at 4 Hz as well as TTP and RT_{50} kinetics at all frequencies. Although cell shortening after CASCs transplantation remained unaltered at 1 and 2 Hz, 4 Hz is considered to be a more physiological relevant frequency in rats. Possible mechanisms by which CASCs restore resident cardiomyocyte contractility are protection of the myocardium from adverse remodeling via paracrine mechanisms, and stimulation of angiogenesis in the infarcted tissue, as described above. In addition, regeneration of cardiac tissue by CASCs can limit infarct expansion, thereby preventing adverse remodeling in adult cardiomyocytes. Altogether, this is the first study investigating the effect of CASCs therapy on resident cardiomyocyte function.

In this study, unloaded cell shortening was only measured in resident cardiomyocytes since no CASCs were detected when excited by a 488 nm laser after cardiomyocyte isolation. However, it was difficult to distinct CASCs from resident cardiomyocytes since resident cardiomyocytes have a lot of autofluorescence when excited with a 488 nm laser. It is also possible that CASCs resided in the Matrigel matrix after transplantation, since Matrigel mimics the native extracellular matrix (ECM). Matrigel is an injectable protein mixture secreted by mouse sarcoma, containing ECM proteins including laminin, collagen IV, heparan sulfate proteoglycans and entactin as well as growth factors such as epidermal growth factor, insulin-like growth factor, TGF-β and fibroblast growth factor. It was shown that Matrigel is a suitable microenvironment for the *in vivo* recruitment of various cell types (73). As such, it is possible that CASCs do not have the tendency to migrate out of the Matrigel matrix, but remained in the Matrigel microenvironment. In addition, enzymatic dissociation of the LV was in this study performed with collagenase type II and protease type XIV. However, isolation of cells from the Matrigel matrix is mainly performed with a dispase or cell recovery solution (BD Biosciences, Erembodegem, Belgium), indicating that Matrigel is poorly digested with a collagenase/protease solution. This suggests that CASCs could not be isolated from Matrigel. Finally, it is possible that CASCs

can migrate out of the Matrigel matrix, but that these cells could not survive the cardiomyocyte isolation procedure, thereby limiting the cell shortening experiments to resident cardiomyocytes.

4.3 CASCs transplantation reduces cardiac fibrosis

The effect of CASCs transplantation on the amount of LV interstitial collagen deposition was assessed by Sirius Red/Fast Green collagen staining of transversal sections. Our results showed that collagen deposition in peri-infarct and LV remote regions was increased in MI animals compared to SHAM animals. This is confirmed by other publications showing an increase in collagen types I, III, IV, V and VI after MI, with types I and III the predominant components in the infarcted region (74). In addition, CASCs transplantation was able to reduce, but not normalize, interstitial collagen deposition. However, statistical significance of data could not be demonstrated due to the limited sample size in the SHAM group. In line with our results, a previous study using CASCs for cardiac repair after MI showed a reduction in scar size 2 months after CASCs transplantation (56). Furthermore, intracardiac transplantation of other stem cells, such as MSCs, significantly reduced cardiac fibrosis (75). The mechanism by which MSCs decreased collagen deposits was attributed to the paracrine effect of MSCs on cardiac myofibroblasts and MMPs, thereby reducing collagen secretion and stimulating ECM protein degradation. However, the mechanisms by which CASCs reduce cardiac collagen content were not investigated yet, but it is suggested that CASCs reduce inflammatory processes and subsequent cardiac fibrosis via paracrine mechanisms. In addition, the angiogenic potential of CASCs may limit infarct expansion and total collagen content, as already described above.

4.4 CASCs engraftment in cardiac tissue is limited

In this study, no CASCs could be identified in LV transversal sections from MI + CASCs animals 4 weeks postoperative, indicating that (A) CASCs engraftment in our study was limited or (B) that we could not identify CASCs due to technical issues. However, *in vivo* and *ex vivo* experiments in our study showed beneficial effects of CASCs therapy on cardiac function 4 weeks after transplantation, suggesting that there is retention of CASCs. Identification of CASCs using a FITC-conjugated anti-GFP antibody was a difficult approach since resident cardiomyocytes show a high degree of autofluorescence when excited with a 488 nm laser. Therefore, the use of an Alexa Fluor 647-conjugated anti-GFP antibody (Invitrogen, A31852, Erembodegem, Belgium) should simplify the distinction of GFP-labeled CASCs with resident cardiac tissue in the future. A previous study investigating CASCs therapy in a mini-pig model of acute MI revealed GFP^+ CASCs in the infarction border zone (56). Engrafted CASCs showed even expression of typical cardiomyocyte proteins such as cTnT, cTnI, Cx43 and MLC-2V, suggesting *in vivo* differentiation of CASCs into ventricular cardiomyocytes. Because CASCs could not be identified

in our study, characterization of *in vivo* differentiated CASCs in LV transversal sections was not performed yet. To investigate whether transplanted CASCs showed cardiomyogenic differentiation, future experiments will be performed on engrafted CASCs to assess expression of typical cardiomyocyte proteins as well as specific players of the excitation-contraction coupling, such as L-type calcium channel subunit α1c, SERCA2a and the ryanodine receptor.

Unfortunately, engraftment of stem cells in cardiac tissue is often limited. Mechanisms underlying low cardiac engraftment include the clearance of stem cells from cardiac tissue via venous or lymphatic drainage, off-target injection into the coronary bloodstream or LV cavity, mechanical extrusion of stem cells from the injection site into the thoracic cavity, or the inability of stem cells to survive and proliferate in the ischemic environment (59). These mechanisms may also contribute to minimal CASCs engraftment observed in our study.

4.5 What is the effect of Matrigel on cardiac repair?

In this study, no MI + Matrigel group was included as control, although this would be the most appropriate control group for the MI + CASCs animals since CASCs were resuspended in Matrigel. The reason for not including this control group is based on a pilot study that was performed in our laboratory (data not shown). Results of the pilot study showed that Matrigel has an effect on cardiac repair, leading to improvement of *in vivo* and *ex vivo* cardiac parameters. This was confirmed by an article investigating the therapeutic efficacy of Matrigel injection in a rat MI model (76). Ou *et al.* showed that Matrigel improved *in vivo* cardiac function by increasing cardiac parameters such as EF, dP/dt_{max} and dP/dt_{min} and by inducing angiogenesis. Moreover, Matrigel injection enhanced the recruitment of c-kit$^+$ (*i.e.* mast cells) and CD34$^+$ cells. It should be noted that CD34 positivity is one of the markers for CASCs isolation, but is often also used as a marker for hematopoietic progenitor and endothelial cells (33). As such, to ensure that a reliable control group was used in this study, no Matrigel was included in the MI control group. However, Matrigel was used as a scaffold in the MI + CASCs group to increase retention of CASCs in the ischemic cardiac environment, since stem cell engraftment in regenerative approaches is rather limited (59). To investigate the effect of CASCs on cardiac repair separately from the effect of Matrigel, two additional groups will be added in a future study: (A) CASCs resuspended in PBS for transplantation after MI and (B) a control group with PBS injection after MI. Nonetheless, the present study cannot conclude whether the improvement in cardiac function is only due to the regenerative potential of CASCs or if it is also a result of the positive effect of Matrigel on cardiac repair.

4.6 Conditioned medium of DPSCs boosts CASCs functional properties *in vitro*

Stem cell therapies for regenerative medicine are often restricted by their low cell engraftment, potentially due to the limited survival and proliferation of stem cells in the injured tissue, as mentioned above (59). To improve CASCs retention in the ischemic environment of the peri-infarct zone of the heart, the stimulatory effect of DPSCs on CASCs proliferation and viability were investigated in an *in vitro* study. Our results showed that CM of DPSCs was able to induce proliferation of CASCs and to protect CASCs from apoptosis *in vitro*. To date, the beneficial effects of DPSCs on cell survival and proliferation were mainly examined in models of neurological disorders, such as spinal cord injury, Alzheimer's disease and retinal injury (77). In a cellular model of Alzheimer's disease established by okadaic acid-induced damage to the human neuroblastoma cell line SH-SY5Y, Wang *et al.* showed that indirect culturing of DPSCs increased cell viability and reduced apoptosis of SH-SY5Y cells (78). However, incubation with CM of DPSCs could not promote SH-SY5Y cell proliferation (79). Furthermore, the protective effect of DPSCs was demonstrated on retinal ganglion cells, as the number of surviving retinal ganglion cells in a rat model of optic nerve damage was increased upon DPSC transplantation (80). In addition, our results showed that DPSCs trigger CASCs migration *in vitro* in a transwell assay. This is in line with the study of Gervois *et al.*, in which SH-SY5Y cells migrated towards CM of DPSCs (79). This suggests that pre-conditioning of CASCs with DPSCs may increase CASCs migratory behavior towards the site of myocardial injury.

All proliferation, viability and migration experiments in this study were performed with the secretome of DPSCs (*i.e.* CM), indicating that no direct cell-cell contacts were necessary to boost CASCs functional properties *in vitro*. It has already been demonstrated that the therapeutic potential of DPSCs is not only attributed to their differentiation capacities, but rather to their strong paracrine properties (81). In this context, Gandia *et al.* implied that the improvement of cardiac function upon intramyocardial injection with DPSCs was due to the strong paracrine nature of DPSCs on the surrounding cardiac tissue (61). Our RT-PCR results indicate that CASCs express the VEGFR1 gene. Although no experiments on VEGFR1 protein expression were performed yet, it suggests that VEGF is an important paracrine agent influencing CASCs behavior. This is confirmed by several studies showing the essential role of VEGF in cell proliferation, migration and survival (82, 83). VEGFR1 functions mainly in the recruitment of progenitor cells, but has only limited effects on cell proliferation. In contrast, vascular endothelial growth factor receptor 2 (VEGFR2) is the predominant receptor in cell migration, proliferation and survival as well as angiogenic signaling (84). Indeed, VEGF released by DPSCs is crucial to induce angiogenesis (85). Therefore, future experiments should also focus on other paracrine, more specifically angiogenic, factors such as insulin-like growth factor-II (IGF-II) and epidermal growth factor

(EGF) and the receptors involved to elucidate the exact mechanisms by which DPSCs can boost CASCs. To summarize, this is the first study investigating the effect of DPSCs on CASCs functional properties, thereby increasing the therapeutic potential of CASCs to truly repair lost cardiac tissue after MI. However, more experiments should be performed on CASCs proliferation and viability to increase sample size. Future experiments on other functional properties of CASCs, such as the effect of DPSCs on CASCs differentiation capacity and angiogenic potential, should also be added. Furthermore, functional experiments should be repeated with neutralizing antibodies to elucidate the mechanisms by which DPSCs can boost CASCs properties.

4.7 Limitations and future perspectives

This study has several limitations that should be noted. No MI + Matrigel group was included as control since a pilot study showed effects of Matrigel on *in vivo* and *ex vivo* cardiac function. To investigate whether CASCs have an effect on cardiac repair separately from Matrigel, a future study will use CASCs resuspended in PBS instead of Matrigel.

It is known that infarct size is often variable in the model of chronic MI used in this study due to technical difficulties in LAD ligation. However, all our data showed the same trend in results, demonstrating reliability of the animal model and indicating that no animals had to be excluded from the analyses.

Functional characterization of *in vivo* differentiated CASCs could not be performed since no CASCs were identified in LV transversal sections and after cardiomyocyte isolation. To characterize functional properties of *in vivo* differentiated CASCs, experiments on CASCs contractile and electrophysiological properties as well as gene and protein expression should be performed 4 weeks after CASCs transplantation. Therefore, another antibody, such as an Alexa Fluor 647-conjugated anti-GFP antibody, should be used to simplify the identification of GFP-labeled CASCs. In addition, isolation of CASCs after being resuspended in PBS should be performed to assess contractile and electrophysiological characteristics.

In this study, echocardiographic views were obtained with a 10 MHz array transducer. It should be noted that it is difficult to detect small differences in cardiac function with this array transducer due to the limited quality of echocardiographic images. It is possible that echocardiographic parameters between groups have small significant differences, but that these were not detected because of the low specificity of the array transducer. Therefore, a new echocardiographic device will be used in the future to detect small differences in cardiac function. In addition, the number of animals used for echocardiographic measurements should be increased, especially in the SHAM and MI + CASCs groups, to assure the reliability of conclusions that are drawn.

LV pressures measured with the pressure catheter were not always accurate, especially in the measurement of minimal LV pressure and EDP. Data of both pressure parameters have negative values because of technical problems with calibration of the minimal pressure. However, minimum diastolic pressures in the LV are physiologically between 0 – 10 mmHg. Because the same catheter was used in all animals and our results are comparable to what was previously published (64), reliability of our results can be confirmed.

In this study, a low yield of intact cardiomyocytes after cell isolation was obtained compared to previous isolations performed in our laboratory. However, data obtained from unloaded cell shortening experiments were comparable to previous results in our group with higher cell yields (86). In addition, cell yield was similar within the three groups, indicating that the observed effects between groups are not biased.

Blood samples were obtained to measure total cTnI levels in plasma samples from SHAM, MI and MI + CASCs animals 24 h after surgery. However, this experiment is not performed yet. A cTnI assay will be performed in the future to assess cardiac function 24 h after MI and CASCs transplantation, since circulating cTn levels are a measure of myocardial cell death.

Finally, more experiments should be performed on interstitial collagen deposition to increase sample size. In addition, more experiments should be performed on the effect of DPSCs on CASCs functional properties and the underlying stimulatory mechanisms, as mentioned above.

5 Conclusion

In this study, we show that CASCs transplantation improves cardiac function after MI both at the organ and cellular level. Taken together, induction of chronic MI leads to cardiac diastolic dysfunction and functional remodeling in surviving cardiomyocytes. Our data indicate that CASCs transplantation is able to improve *in vivo* systolic and diastolic cardiac function. In addition, we show that CASCs therapy can restore resident cardiomyocyte shortening and kinetics. Furthermore, CASCs transplantation reduces cardiac fibrosis after MI. However, no CASCs were identified in cardiac tissue, indicating limited CASCs engraftment. As such, functional properties of *in vivo* differentiated CASCs could not be assessed in this study. Additionally, this is the first study investigating the effect of DPSCs on CASCs functional properties. We demonstrate that DPSCs can boost CASCs proliferation, viability and migration, in which VEGFR1 signaling may be involved. To summarize, this study shows the efficacy of CASCs therapy after MI.

6 References

1. World Health Organization. The top 10 causes of death 2018 [Available from: http://www.who.int/news-room/fact-sheets/detail/the-top-10-causes-of-death.
2. Rhee J.W., Sabatine M.S., Lilly L.S. Ischemic Heart Disease. In: Lilly L.S., editor. Pathophysiology of Heart Disease. 5 ed. Baltimore: Lippincott Williams & Wilkins, a Wolters Kluwer business; 2011. p. 135-60.
3. Thygesen K, Alpert JS, Jaffe AS, Chaitman BR, Bax JJ, Morrow DA, et al. Fourth Universal Definition of Myocardial Infarction (2018). Journal of the American College of Cardiology. 2018;72(18):2231-64.
4. Reddy K, Khaliq A, Henning RJ. Recent advances in the diagnosis and treatment of acute myocardial infarction. World journal of cardiology. 2015;7(5):243-76.
5. Ibanez B, James S, Agewall S, Antunes MJ, Bucciarelli-Ducci C, Bueno H, et al. 2017 ESC Guidelines for the management of acute myocardial infarction in patients presenting with ST-segment elevation. Kardiologia polska. 2018;76(2):229-313.
6. Forouzanfar MH, Moran AE, Flaxman AD, Roth G, Mensah GA, Ezzati M, et al. Assessing the global burden of ischemic heart disease, part 2: analytic methods and estimates of the global epidemiology of ischemic heart disease in 2010. Global heart. 2012;7(4):331-42.
7. Anand SS, Islam S, Rosengren A, Franzosi MG, Steyn K, Yusufali AH, et al. Risk factors for myocardial infarction in women and men: insights from the INTERHEART study. European heart journal. 2008;29(7):932-40.
8. Bagai A, Alexander KP, Berger JS, Senior R, Sajeev C, Pracon R, et al. Use of troponin assay 99th percentile as the decision level for myocardial infarction diagnosis. American heart journal. 2017;190:135-9.
9. Frangogiannis NG. Pathophysiology of Myocardial Infarction. Comprehensive Physiology. 2015;5(4):1841-75.
10. Bentzon JF, Otsuka F, Virmani R, Falk E. Mechanisms of plaque formation and rupture. Circulation research. 2014;114(12):1852-66.
11. Prabhu SD, Frangogiannis NG. The Biological Basis for Cardiac Repair After Myocardial Infarction: From Inflammation to Fibrosis. Circulation research. 2016;119(1):91-112.
12. Chatterjee N.A., Fifer M.A. Heart Failure. In: Lilly L.S., editor. Pathophysiology of Heart Disease. 5 ed. Baltimore: Lippincott Williams & Wilkins, a Wolters Kluwer business; 2011. p. 216-43.
13. Bhatt AS, Ambrosy AP, Velazquez EJ. Adverse Remodeling and Reverse Remodeling After Myocardial Infarction. Current cardiology reports. 2017;19(8):71.
14. Sackner-Bernstein JD. The myocardial matrix and the development and progression of ventricular remodeling. Current cardiology reports. 2000;2(2):112-9.
15. Cannon CP, Weintraub WS, Demopoulos LA, Vicari R, Frey MJ, Lakkis N, et al. Comparison of early invasive and conservative strategies in patients with unstable coronary syndromes treated with the glycoprotein IIb/IIIa inhibitor tirofiban. The New England journal of medicine. 2001;344(25):1879-87.
16. Kumar A, Cannon CP. Acute coronary syndromes: diagnosis and management, part I. Mayo Clinic proceedings. 2009;84(10):917-38.
17. de Jonge N, Kirkels JH, Klopping C, Lahpor JR, Caliskan K, Maat AP, et al. Guidelines for heart transplantation. Netherlands heart journal : monthly journal of the Netherlands Society of Cardiology and the Netherlands Heart Foundation. 2008;16(3):79-87.
18. Bergmann O, Bhardwaj RD, Bernard S, Zdunek S, Barnabe-Heider F, Walsh S, et al. Evidence for cardiomyocyte renewal in humans. Science (New York, NY). 2009;324(5923):98-102.
19. Beltrami AP, Urbanek K, Kajstura J, Yan SM, Finato N, Bussani R, et al. Evidence that human cardiac myocytes divide after myocardial infarction. The New England journal of medicine. 2001;344(23):1750-7.
20. Katarzyna R. Adult Stem Cell Therapy for Cardiac Repair in Patients After Acute Myocardial Infarction Leading to Ischemic Heart Failure: An Overview of Evidence from the Recent Clinical Trials. Current cardiology reviews. 2017;13(3):223-31.

21. Pavo N, Charwat S, Nyolczas N, Jakab A, Murlasits Z, Bergler-Klein J, et al. Cell therapy for human ischemic heart diseases: critical review and summary of the clinical experiences. Journal of molecular and cellular cardiology. 2014;75:12-24.
22. Deutsch MA, Sturzu A, Wu SM. At a crossroad: cell therapy for cardiac repair. Circulation research. 2013;112(6):884-90.
23. Chiu RC, Zibaitis A, Kao RL. Cellular cardiomyoplasty: myocardial regeneration with satellite cell implantation. The Annals of thoracic surgery. 1995;60(1):12-8.
24. Smits PC, van Geuns RJ, Poldermans D, Bountioukos M, Onderwater EE, Lee CH, et al. Catheter-based intramyocardial injection of autologous skeletal myoblasts as a primary treatment of ischemic heart failure: clinical experience with six-month follow-up. Journal of the American College of Cardiology. 2003;42(12):2063-9.
25. Durrani S, Konoplyannikov M, Ashraf M, Haider KH. Skeletal myoblasts for cardiac repair. Regenerative medicine. 2010;5(6):919-32.
26. Menasche P, Alfieri O, Janssens S, McKenna W, Reichenspurner H, Trinquart L, et al. The Myoblast Autologous Grafting in Ischemic Cardiomyopathy (MAGIC) trial: first randomized placebo-controlled study of myoblast transplantation. Circulation. 2008;117(9):1189-200.
27. Reinecke H, MacDonald GH, Hauschka SD, Murry CE. Electromechanical coupling between skeletal and cardiac muscle. Implications for infarct repair. The Journal of cell biology. 2000;149(3):731-40.
28. Hendrikx M, Hensen K, Clijsters C, Jongen H, Koninckx R, Bijnens E, et al. Recovery of regional but not global contractile function by the direct intramyocardial autologous bone marrow transplantation: results from a randomized controlled clinical trial. Circulation. 2006;114(1 Suppl):I101-7.
29. Lunde K, Solheim S, Aakhus S, Arnesen H, Abdelnoor M, Egeland T, et al. Intracoronary injection of mononuclear bone marrow cells in acute myocardial infarction. The New England journal of medicine. 2006;355(12):1199-209.
30. Gruh I, Beilner J, Blomer U, Schmiedl A, Schmidt-Richter I, Kruse ML, et al. No evidence of transdifferentiation of human endothelial progenitor cells into cardiomyocytes after coculture with neonatal rat cardiomyocytes. Circulation. 2006;113(10):1326-34.
31. Koninckx R, Hensen K, Daniels A, Moreels M, Lambrichts I, Jongen H, et al. Human bone marrow stem cells co-cultured with neonatal rat cardiomyocytes display limited cardiomyogenic plasticity. Cytotherapy. 2009;11(6):778-92.
32. Murry CE, Soonpaa MH, Reinecke H, Nakajima H, Nakajima HO, Rubart M, et al. Haematopoietic stem cells do not transdifferentiate into cardiac myocytes in myocardial infarcts. Nature. 2004;428(6983):664-8.
33. Le Blanc K, Mougiakakos D. Multipotent mesenchymal stromal cells and the innate immune system. Nature reviews Immunology. 2012;12(5):383-96.
34. Chamberlain G, Fox J, Ashton B, Middleton J. Concise review: mesenchymal stem cells: their phenotype, differentiation capacity, immunological features, and potential for homing. Stem cells (Dayton, Ohio). 2007;25(11):2739-49.
35. Hare JM, Fishman JE, Gerstenblith G, DiFede Velazquez DL, Zambrano JP, Suncion VY, et al. Comparison of allogeneic vs autologous bone marrow-derived mesenchymal stem cells delivered by transendocardial injection in patients with ischemic cardiomyopathy: the POSEIDON randomized trial. Jama. 2012;308(22):2369-79.
36. Heldman AW, DiFede DL, Fishman JE, Zambrano JP, Trachtenberg BH, Karantalis V, et al. Transendocardial mesenchymal stem cells and mononuclear bone marrow cells for ischemic cardiomyopathy: the TAC-HFT randomized trial. Jama. 2014;311(1):62-73.
37. Hendrikx M, Fanton Y, Willems L, Daniels A, Declercq J, Windmolders S, et al. From Bone Marrow to Cardiac Atrial Appendage Stem Cells for Cardiac Repair: A Review. Current medicinal chemistry. 2016;23(23):2421-38.
38. Takahashi K, Yamanaka S. Induction of pluripotent stem cells from mouse embryonic and adult fibroblast cultures by defined factors. Cell. 2006;126(4):663-76.

39. Nelson TJ, Martinez-Fernandez A, Yamada S, Perez-Terzic C, Ikeda Y, Terzic A. Repair of acute myocardial infarction by human stemness factors induced pluripotent stem cells. Circulation. 2009;120(5):408-16.
40. Pawani H, Bhartiya D. Pluripotent stem cells for cardiac regeneration: overview of recent advances & emerging trends. The Indian journal of medical research. 2013;137(2):270-82.
41. Laugwitz KL, Moretti A, Lam J, Gruber P, Chen Y, Woodard S, et al. Postnatal isl1+ cardioblasts enter fully differentiated cardiomyocyte lineages. Nature. 2005;433(7026):647-53.
42. Oh H, Bradfute SB, Gallardo TD, Nakamura T, Gaussin V, Mishina Y, et al. Cardiac progenitor cells from adult myocardium: homing, differentiation, and fusion after infarction. Proceedings of the National Academy of Sciences of the United States of America. 2003;100(21):12313-8.
43. Martin CM, Meeson AP, Robertson SM, Hawke TJ, Richardson JA, Bates S, et al. Persistent expression of the ATP-binding cassette transporter, Abcg2, identifies cardiac SP cells in the developing and adult heart. Developmental biology. 2004;265(1):262-75.
44. Bearzi C, Rota M, Hosoda T, Tillmanns J, Nascimbene A, De Angelis A, et al. Human cardiac stem cells. Proceedings of the National Academy of Sciences of the United States of America. 2007;104(35):14068-73.
45. Koninckx R, Daniels A, Windmolders S, Mees U, Macianskiene R, Mubagwa K, et al. The cardiac atrial appendage stem cell: a new and promising candidate for myocardial repair. Cardiovascular research. 2013;97(3):413-23.
46. Bolli R, Chugh AR, D'Amario D, Loughran JH, Stoddard MF, Ikram S, et al. Cardiac stem cells in patients with ischaemic cardiomyopathy (SCIPIO): initial results of a randomised phase 1 trial. Lancet (London, England). 2011;378(9806):1847-57.
47. Reardon S. US government halts heart stem-cell study. Nature News & Comment. 2018.
48. van Berlo JH, Kanisicak O, Maillet M, Vagnozzi RJ, Karch J, Lin SC, et al. c-kit+ cells minimally contribute cardiomyocytes to the heart. Nature. 2014;509(7500):337-41.
49. Pouly J, Bruneval P, Mandet C, Proksch S, Peyrard S, Amrein C, et al. Cardiac stem cells in the real world. The Journal of thoracic and cardiovascular surgery. 2008;135(3):673-8.
50. Messina E, De Angelis L, Frati G, Morrone S, Chimenti S, Fiordaliso F, et al. Isolation and expansion of adult cardiac stem cells from human and murine heart. Circulation research. 2004;95(9):911-21.
51. Malliaras K, Makkar RR, Smith RR, Cheng K, Wu E, Bonow RO, et al. Intracoronary cardiosphere-derived cells after myocardial infarction: evidence of therapeutic regeneration in the final 1-year results of the CADUCEUS trial (CArdiosphere-Derived aUtologous stem CElls to reverse ventricULar dySfunction). Journal of the American College of Cardiology. 2014;63(2):110-22.
52. Andersen DC, Andersen P, Schneider M, Jensen HB, Sheikh SP. Murine "cardiospheres" are not a source of stem cells with cardiomyogenic potential. Stem cells (Dayton, Ohio). 2009;27(7):1571-81.
53. Corti S, Locatelli F, Papadimitriou D, Donadoni C, Salani S, Del Bo R, et al. Identification of a primitive brain-derived neural stem cell population based on aldehyde dehydrogenase activity. Stem cells (Dayton, Ohio). 2006;24(4):975-85.
54. Gentry T, Foster S, Winstead L, Deibert E, Fiordalisi M, Balber A. Simultaneous isolation of human BM hematopoietic, endothelial and mesenchymal progenitor cells by flow sorting based on aldehyde dehydrogenase activity: implications for cell therapy. Cytotherapy. 2007;9(3):259-74.
55. Moreb JS. Aldehyde dehydrogenase as a marker for stem cells. Current stem cell research & therapy. 2008;3(4):237-46.
56. Fanton Y, Robic B, Rummens JL, Daniels A, Windmolders S, Willems L, et al. Cardiac atrial appendage stem cells engraft and differentiate into cardiomyocytes in vivo: A new tool for cardiac repair after MI. International journal of cardiology. 2015;201:10-9.
57. Fanton Y, Houbrechts C, Willems L, Daniels A, Linsen L, Ratajczak J, et al. Cardiac atrial appendage stem cells promote angiogenesis in vitro and in vivo. Journal of molecular and cellular cardiology. 2016;97:235-44.
58. Menasche P. Stem cell therapy for heart failure: are arrhythmias a real safety concern? Circulation. 2009;119(20):2735-40.

59. Kanda P, Davis DR. Cellular mechanisms underlying cardiac engraftment of stem cells. Expert opinion on biological therapy. 2017;17(9):1127-43.
60. Gronthos S, Mankani M, Brahim J, Robey PG, Shi S. Postnatal human dental pulp stem cells (DPSCs) in vitro and in vivo. Proceedings of the National Academy of Sciences of the United States of America. 2000;97(25):13625-30.
61. Gandia C, Arminan A, Garcia-Verdugo JM, Lledo E, Ruiz A, Minana MD, et al. Human dental pulp stem cells improve left ventricular function, induce angiogenesis, and reduce infarct size in rats with acute myocardial infarction. Stem cells (Dayton, Ohio). 2008;26(3):638-45.
62. Song M, Jue SS, Cho YA, Kim EC. Comparison of the effects of human dental pulp stem cells and human bone marrow-derived mesenchymal stem cells on ischemic human astrocytes in vitro. Journal of neuroscience research. 2015;93(6):973-83.
63. Hilkens P, Fanton Y, Martens W, Gervois P, Struys T, Politis C, et al. Pro-angiogenic impact of dental stem cells in vitro and in vivo. Stem cell research. 2014;12(3):778-90.
64. Deluyker D, Ferferieva V, Driesen RB, Verboven M, Lambrichts I, Bito V. Pyridoxamine improves survival and limits cardiac dysfunction after MI. Scientific reports. 2017;7(1):16010.
65. Delicce AV, Makaryus AN. Physiology, Frank Starling Law. StatPearls. Treasure Island (FL): StatPearls Publishing LLC.; 2019.
66. Gabriel-Costa D. The pathophysiology of myocardial infarction-induced heart failure. Pathophysiology : the official journal of the International Society for Pathophysiology. 2018;25(4):277-84.
67. Hou J, Wang L, Jiang J, Zhou C, Guo T, Zheng S, et al. Cardiac stem cells and their roles in myocardial infarction. Stem cell reviews. 2013;9(3):326-38.
68. Broughton KM, Wang BJ, Firouzi F, Khalafalla F, Dimmeler S, Fernandez-Aviles F, et al. Mechanisms of Cardiac Repair and Regeneration. Circulation research. 2018;122(8):1151-63.
69. Hare JM, Traverse JH, Henry TD, Dib N, Strumpf RK, Schulman SP, et al. A randomized, double-blind, placebo-controlled, dose-escalation study of intravenous adult human mesenchymal stem cells (prochymal) after acute myocardial infarction. Journal of the American College of Cardiology. 2009;54(24):2277-86.
70. Florea V, Rieger AC, DiFede DL, El-Khorazaty J, Natsumeda M, Banerjee MN, et al. Dose Comparison Study of Allogeneic Mesenchymal Stem Cells in Patients With Ischemic Cardiomyopathy (The TRIDENT Study). Circulation research. 2017;121(11):1279-90.
71. Loennechen JP, Wisloff U, Falck G, Ellingsen O. Cardiomyocyte contractility and calcium handling partially recover after early deterioration during post-infarction failure in rat. Acta physiologica Scandinavica. 2002;176(1):17-26.
72. Bito V, de Waard MC, Biesmans L, Lenaerts I, Ozdemir S, van Deel E, et al. Early exercise training after myocardial infarction prevents contractile but not electrical remodelling or hypertrophy. Cardiovascular research. 2010;86(1):72-81.
73. Grimaldi A, Bianchi C, Greco G, Tettamanti G, Noonan DM, Valvassori R, et al. In vivo isolation and characterization of stem cells with diverse phenotypes using growth factor impregnated biomatrices. PloS one. 2008;3(4):e1910.
74. Li L, Zhao Q, Kong W. Extracellular matrix remodeling and cardiac fibrosis. Matrix biology : journal of the International Society for Matrix Biology. 2018;68-69:490-506.
75. Mias C, Lairez O, Trouche E, Roncalli J, Calise D, Seguelas MH, et al. Mesenchymal stem cells promote matrix metalloproteinase secretion by cardiac fibroblasts and reduce cardiac ventricular fibrosis after myocardial infarction. Stem cells (Dayton, Ohio). 2009;27(11):2734-43.
76. Ou L, Li W, Zhang Y, Wang W, Liu J, Sorg H, et al. Intracardiac injection of matrigel induces stem cell recruitment and improves cardiac functions in a rat myocardial infarction model. Journal of cellular and molecular medicine. 2011;15(6):1310-8.
77. Luo L, He Y, Wang X, Key B, Lee BH, Li H, et al. Potential Roles of Dental Pulp Stem Cells in Neural Regeneration and Repair. Stem cells international. 2018;2018:1731289.
78. Wang F, Jia Y, Liu J, Zhai J, Cao N, Yue W, et al. Dental pulp stem cells promote regeneration of damaged

neuron cells on the cellular model of Alzheimer's disease. Cell biology international. 2017;41(6):639-50.
79. Gervois P, Wolfs E, Dillen Y, Hilkens P, Ratajczak J, Driesen RB, et al. Paracrine Maturation and Migration of SH-SY5Y Cells by Dental Pulp Stem Cells. Journal of dental research. 2017;96(6):654-62.
80. Mead B, Logan A, Berry M, Leadbeater W, Scheven BA. Dental pulp stem cells, a paracrine-mediated therapy for the retina. Neural regeneration research. 2014;9(6):577-8.
81. Leong WK, Henshall TL, Arthur A, Kremer KL, Lewis MD, Helps SC, et al. Human adult dental pulp stem cells enhance poststroke functional recovery through non-neural replacement mechanisms. Stem cells translational medicine. 2012;1(3):177-87.
82. Wang S, Li X, Parra M, Verdin E, Bassel-Duby R, Olson EN. Control of endothelial cell proliferation and migration by VEGF signaling to histone deacetylase 7. Proceedings of the National Academy of Sciences of the United States of America. 2008;105(22):7738-43.
83. Zhang L, Wang JN, Tang JM, Kong X, Yang JY, Zheng F, et al. VEGF is essential for the growth and migration of human hepatocellular carcinoma cells. Molecular biology reports. 2012;39(5):5085-93.
84. Cebe-Suarez S, Zehnder-Fjallman A, Ballmer-Hofer K. The role of VEGF receptors in angiogenesis; complex partnerships. Cellular and molecular life sciences : CMLS. 2006;63(5):601-15.
85. Bronckaers A, Hilkens P, Fanton Y, Struys T, Gervois P, Politis C, et al. Angiogenic properties of human dental pulp stem cells. PloS one. 2013;8(8):e71104.
86. Deluyker D, Evens L, Belien H, Bito V. Acute exposure to glycated proteins reduces cardiomyocyte contractile capacity. Experimental physiology. 2019.